CENTRE FOR
SYSTEMS
SCIENCE

Simon Fraser University, Burnaby, B.C., Canada V5A 1S6 / (604) 291-4704

92-05404/

Passive Dynamic Walking

Tad McGeer

CSS-IS TR 88-02

Symbols

(defining equations are noted in parentheses)

Upper case

$\mathbf{D}_{\theta\theta}$, $\mathbf{D}_{\theta\Omega}$, $\mathbf{D}_{\Omega\theta}$, $\mathbf{D}_{\Omega\Omega}$	start-of-step to end-of-step transition submatrix (22, 23)
$\nabla\mathbf{D}_{\theta\theta}$, $\nabla\mathbf{D}_{\theta\Omega}$, $\nabla\mathbf{D}_{\Omega\theta}$, $\nabla\mathbf{D}_{\Omega\Omega}$	derivatives of **D** *w.r.t.* step period (29)
$\mathbf{D}'$	(26)
$\mathbf{F}$	damping matrix (38)
H	angular momentum (A3)
$\mathbf{I}$	identity matrix
J	link moment of inertia about its mass centre
$\mathbf{M}$	inertia matrix for an N-link chain (14, A16)
M	element of **M** (A16)
N	number of chain links
R	foot radius/leg length
$\mathbf{S}$	transition matrix for linearised step-to-step equations (31)
T	torque
$\vec{V}$	link velocity vector (A7)

Lower case

$\vec{b}'$	derivative of chain equilibrium angles *w.r.t.* slope (17, A15)
c	distance from proximal joint to link mass centre (figure 17)
d	distance from distal joint to link mass centre (figure 17)
f	viscous friction coefficient (38)
g	gravitational acceleration
l	link length (figure 17)
m	mass
m_{HIP}	point mass at the hip joint
r_{gyr}	leg radius of gyration/leg length
$\vec{r}_{np}$	position vector from joint n to mass centre of link p (figure 16)
w	offset from link axis to mass centre (figure 17)
$\hat{x}$, $\hat{y}$	unit vectors (figure 17)
z	eigenvalue of linearised step-to-step equations (31)

Greek

α	hip half-angle at support transfer (figure 6)
γ	slope (figure 4)
η	ratio of speeds across support transfer (5)
θ	link angle (figure 17)
$\Delta\theta$	perturbation in θ from the surface normal (figure 3)
Λ	support transfer matrix (19)
$\nabla\Lambda$	derivative of Λ *w.r.t.* α
$\vec{\chi}$	(33)
σ	timescale parameter for the rimless wheel (2)
τ	dimensionless time $t\sqrt{g/l}$
τ_k	period of k^{th} step
Ω	angular speed
ω	frequency
ω_{LR}	frequency of lateral rocking

Subscripts

0	steady-cycling condition
C	stance ("contact") leg
F	swing ("free") leg
k	as in k^{th} step
n, *p*	link indices, 1 for the contact link
SE	static equilibrium
W	due to offset between mass centre and link axis

19 May 1988

PASSIVE DYNAMIC WALKING

Tad McGeer

School of Engineering Science
Simon Fraser University
Burnaby, British Columbia, Canada V5A 1S6
(TMCG@sfu.MAILNET)

Abstract

There exists a class of two-legged machines for which walking is a natural dynamic mode: Once started on a shallow slope, such a machine will settle into a steady gait quite comparable to human walking, without active control or energy input. Interpretation and analysis of the underlying physics is straightforward; the walking cycle, its stability, and sensitivity to parameter variations are easily calculated. Experiments with a test machine verify that the passive walking effect can be readily exploited in practice. While the dynamics are most clearly demonstrated by an unpowered machine, they also promise to make powered walkers efficient, dextrous, and easily controlled.

1. Introduction

1.1. Static *vs* Dynamic

Research on legged locomotion is motivated partly by fundamental curiousity about its mechanics, and partly by the practical utility of machines capable of traversing uneven surfaces. Increasing general interest in robotics in recent years has coincided with the appearance of a wide variety of legged machines. A brief classification of these machines will indicate where our own work fits in. First one should distinguish between *static* and *dynamic* machines. The former maintain static equilibrium throughout their motion. This requires at least four legs, and more commonly six. It also imposes a speed limit, since cyclic accelerations must be limited in order

to minimise inertial effects. Outstanding examples of static walkers are the Odex series (Russell, 1983) and the Adaptive Suspension Vehicle (Waldron, 1986). Dynamic machines, on the other hand, are more like people; they can have fewer legs than static machines, and are potentially faster and more dextrous.

1.2. Dynamics *vs* Control

Our interest is in dynamic walking machines, which for our purposes can be classified according to the role of active control in generating the gait. At one end of the spectrum is the biped walker by Mita et al (1984), in which the motion is generated *entirely* by linear feedback control: At the end of one step, the controller commands joint angles for the end of the next step, and attempts to null the errors. There is no explicit specification of the motion between these end conditions. Yamada, Furusho, and Sano (1985) took an approach which also relies heavily on feedback, although in this case it is used to track specified joint *trajectories* rather than just the end points. Also, the stance leg is left free to rotate as an inverted pendulum, which, as we shall discuss, is a key element of "natural" walking.

In Miura's (1984) machines, the basic gait is generated by active control as well, but in the form of a *precalculated* control schedule rather than feedback. Again the stance leg is left free. Since the precalculated control inputs cannot compensate for modelling errors and disturbances, small feedback corrections are used to maintain the desired walking cycle. Most significantly, these corrections are not applied continuously throughout the motion. Instead, the precalculated step is treated as a processor whose output, the end-of-step state of the machine, can be adjusted simply by changing the input, the beginning-of-step state. Thus the feedback controller responds to an error in the gait by modifying initial conditions for subsequent steps, and so over several steps the error is eliminated. In this paper you will see analysis of a similar process. Raibert (1986) has developed comparable ideas in a somewhat purer form, and applied them with great success to dynamic machines having from one to four legs. Actually these are classified as runners rather than walkers, since the machines are in free flight for part of each stride.

All of these machines require some form of active control to generate the gait; when the power stops, they fall over. However, I've ordered them according to the style of implementa-

tion, ranging from continuous active feedback to once-per-step adjustment of an actively generated but nevertheless *fixed* cycle. This paper discusses a machine at the extreme end of the spectrum: Gravity and natural dynamics alone generate the walking cycle, which we therefore call "passive walking." Active input is necessary only to modify the cycle, as in turning or changing speed.

1.3. Motivation for Passive Walking

The practical motivation for studying passive walking is, first, that it makes for mechanical simplicity and relatively high efficiency. (The specific resistance of our machine is somewhat better than 0.02 in a comfortable stride.) Second, control of speed and direction is simplified when one doesn't have to worry about the details of generating the gait. Moreover, the simplicity of the machine promotes understanding. Consider an analogy with the development of powered flight: The Wrights put their initial efforts into studying gliders, as did their predecessors Cayley and Lilienthal. Once they had a reasonable grasp of dynamics and control, adding a powerplant was a relatively minor modification. (In fact their engine wasn't very good for its day, but their other strengths led them to outstanding success.) As I'll explain, adding power to a passive walker involves a comparably minor modification.

In fact, passive walkers existed long before contemporary research machines. Figure 1 shows a biped toy which walks on shallow slopes, while rocking from side to side to raise the swing foot above the ground. A similar quadruped toy walks on the flat while being pulled by a dangling weight. Figure 1 is actually from a paper by McMahon (1984), which points out that human walking is also at least quasi-passive: Both physiology and physics indicate that no input is supplied to the leg during its swing phase. Our test machine, shown in figures 2 and 3, can be regarded as a two-dimensional version of the toy. It has similar dynamics in the longitudinal plane, but does not rock sideways. Instead on each step small motors retract the swing feet just far enough to clear the ground. In comparison with the toy's fully passive dynamics, our use of active retraction is less elegant. However, it is an expedient which allows us to concentrate on passive walking in the simplest two-dimensional form. (Parameters of the machine are listed in table 1.)

Table 1
Parameters of the experimental machine

mass of each leg	$1.94kg$
leg length with foot extended, l	$0.53m$
foot radius/leg length (R)	0.33
radius of gyration/leg length (r_{gyr})	0.32
centre of mass height/leg length (c)	0.63
offset from centre of mass to leg axis (w)	
outer leg pair	+0.008
centre leg	-0.01

Note that the values for c and w are specified using the convention for the stance leg, shown in figure 17.

1.4. Outline of the Paper

I will begin discussion of passive walking with two simple models to illustrate energetics and dynamics. Then I will develop an analysis of passive walking for a two-dimensional biped, that is, one which has no lateral motion. (Our machine is specifically prevented from lateral motion: It walks like a person on crutches, centre leg alternating with paired outer legs.) The analysis includes solution for the steady gait, and for the step-to-step stability of that gait. Once the theory is in hand, I will use it to study parameter variations, and to review parameter selection for the test machine. Next I will discuss our initial experiments. The paper ends with some comments on developments to come, including passive foot clearance, steering, gait variation, and addition of power.

2. Illustrative Contrivances

2.1. A Rimless Wagon Wheel

A rimless wheel, figure 4, is useful for illustrating the energetics of walking, and some concepts which appear in analysis of a biped. The wheel will roll downhill at a steady speed, with gravity balancing the angular momentum lost on each support transfer. The forward speed can

be calculated as follows: First relate the *angular* speed at the start of a step (*i.e.* with the leg at $\theta = -\alpha_0$) to the speed at the end of the step ($\theta = \alpha_0$). Next calculate the change in speed when support is transferred to the next leg. Then impose the condition that the process must be cyclic. The analysis is simplest when cast in dimensionless terms, with total mass m, leg length l, and characteristic time $\sqrt{l/g}$ providing the base units.

We begin with equations of motion linearised about $\theta = 0$. This is an acceptable restriction for us, since the small-angle approximation is quite good in the range of comfortable walking. The equation of motion during the step, then, can be treated as

$$\frac{d^2\theta}{d\tau^2} - \sigma^2 \theta = \sigma^2 \gamma \tag{1}$$

σ is the dimensionless timescale parameter:

$$\sigma^2 = \frac{1}{1 + r_{gyr}^2} \tag{2}$$

At the end of the step (say time τ_0), support is transferred to the next leg. This is approximated as an instantaneous event. That is, the next leg strikes the ground in a perfectly inelastic collision. Then angular momentum about the point of collision is conserved. Thus immediately *before* the collision, this angular momentum is

$$H^- = (\cos 2\alpha_0 + r_{gyr}^2)\, ml^2\, \Omega^- \tag{3}$$

After the collision, it is simply

$$H^+ = (1 + r_{gyr}^2)\, ml^2\, \Omega^+ \tag{4}$$

Equating these gives the ratio of angular speeds before and after the collision:

$$\frac{\Omega^+}{\Omega^-} = \frac{\cos 2\alpha_0 + r_{gyr}^2}{1 + r_{gyr}^2} = 1 - \sigma^2 (1 - \cos 2\alpha_0) \triangleq \eta \tag{5}$$

Note that the ratio tends toward unity with smaller leg separation and larger inertia.

The walking cycle is steady if the velocity after support transfer (say Ω_0) repeats from step to step. Thus the steady step has the following initial and final states:

$$\theta(0) = -\alpha_0 \quad \Omega(0) = \Omega_0$$

$$\theta(\tau_0) = \alpha_0 \quad \Omega(\tau_0) = \frac{\Omega_0}{\eta} \tag{6}$$

To solve for Ω_0 and τ_0, invoke the equation of motion (1). Its solution has the form

$$\theta(\tau) = Ae^{\sigma\tau} + Be^{-\sigma\tau} \tag{7}$$

Imposing the four conditions (6) provides the four equations necessary to find Ω_0, τ_0, A, and B. The results are

$$\Omega_0 = \sqrt{\frac{4\gamma\alpha_0\sigma^2\eta^2}{1-\eta^2}} \tag{8}$$

$$e^{\sigma\tau_0} = \frac{\gamma+\alpha_0+\dfrac{\Omega_0}{\sigma\eta}}{\gamma-\alpha_0+\dfrac{\Omega_0}{\sigma}} \tag{9}$$

The last formula provides the information necessary for calculating the *forward* speed, which in dimensionless terms, and for small α_0, is

$$V \approx \frac{2\alpha_0}{\tau_0} \tag{10}$$

This is plotted in figure 5 as a function of the slope.

An additional question to be addressed is stability: If Ω is initially different from Ω_0, will the motion converge to the steady cycle? The answer, obtained by extention of this analysis, turns out to be yes. I will discuss stability in more detail later in the paper.

An example will provide some feel for the motion. Take $\gamma = 0.02$, $l = 0.5m$, $\alpha_0 = 0.3$, and $\sigma = 0.75$ (which implies $\eta \approx 0.90$). The corresponding speed is $0.36m/s$. This is comparable with the speed of a biped with the same stride and leg length (table 3 and figure 8).

2.2. Reinventing the Wheel

The rimless wheel is a legged machine of sorts, but its legs are not well utilised. One would like to eliminate all but two, by arranging for the free leg to swing forward in just the right way so that it can pick up the next step. Figure 6 shows a simple model which illustrates the necessary dynamics. It includes only two spokes of the wheel, each in this case having a section of rim, and a pin joint at the hip.

Figure 7 is a plot of the desired motion. At the beginning of the step, the legs should have

opposite angles and equal speeds. (I will use subscript "*C*" for the stance, or "contact" leg, and "*F*" for the swing, or "free" leg; thus initial conditions for the step are $\theta_F = -\theta_C = \alpha_0$; $\Omega_F = \Omega_C = \Omega_0$). During the step, the free leg swings ahead of the stance leg; the step ends when they have exchanged angles. (Note that while in this model the "free" foot remains tangent to the ground throughout the swing, in practice it is kept clear of the ground - by lateral rocking in the toys, and by active retraction in our test machine.) *If* as the angles reach $\pm\alpha_0$ the speeds of the legs happen to be exactly equal, then support can just roll from one rim to the next without any change in angular momentum. Thus the cycle can repeat, without loss of energy.

Analysis of the cycle is simple if the hip mass is much larger than the leg mass and is concentrated at the hip. In that case the stance leg is not affected by the motion of the swing leg, and it becomes just a section of wheel rolling at constant speed. In turn, therefore, since the hub is not accelerated, the swing leg is an *unforced* pendulum. Then the period of the step is just the time required for a sinusoid, as in figure 7, to swing from some initial angle and speed to the *opposite* angle and the *same* speed. This turns out to satisfy

$$\sin \omega_F \tau_0 = -\frac{\omega_F \tau_0}{2} (1 + \cos \omega_F \tau_0) \Rightarrow \omega_F \tau_0 = 4.058 \qquad (11)$$

Thus the step period is about 2/3 the pendulum period of the swing leg. This conclusion involves the small-angle approximation, but apart from that, notice that the period is independent of the hip half-angle α_0. So according to (10), changing the forward speed involves a change not in timing, but rather in amplitude, of the natural walking cycle. Thus a synthetic wheel, like an ordinary (albeit frictionless) wheel, can roll at arbitrary speed on a flat surface. Since the machine is equally comfortable at all speeds, it is neutrally stable at any one speed.

We will now delve into analysis of the more general biped of figure 3. The modelling is somewhat more complicated than in these two introductory examples, but you will see similar mechanisms at work in the results (figures 8-13).

3. General Two-dimensional Biped Analysis

3.1. Layout of a Two-dimensional Biped

Our general biped (figure 3) offers much more flexibility in parameter selection that the simple synthetic wheel. An important new feature is smaller feet. They remain circular in section, but their radius need not be equal to the leg length. Smaller radius affects both kinematics and dynamics; the point to note about kinematics is that both legs are in contact *only* when $\theta_C = \pm\theta_F$. Therefore, *provided* the swing foot is lifted briefly as the legs pass through the vertical, support transfer *will* occur at the desired end-of-step point as shown in figure 7. (For the synthetic wheel support could be transferred with the legs at any angle.) For the purposes of this analysis one needn't address how foot clearance is arranged, except to impose the condition that it should not entail a significant change in leg inertia.

The model for support transfer remains an impulsive inelastic collision, as for the rimless wheel. At first we had some doubt about the validity of this approximation, particularly because the feet might slip. As a preventative measure we have used roughened rubber soles in the feet of the test machine. These don't appear to slip at all, and support transfer is certainly signalled by a very impulsive noise. There are discrepancies between the predicted and measured gaits which may be due to somewhat elastic support transfer, but the impulsive model is certainly a good approximation.

In its simplest form, the "general" biped is fully specified by only three parameters: dimensionless foot radius R, centre of mass height c, and leg radius of gyration r_{gyr}. A more elaborate model also provides for mass centres offset from the leg axis, for mismatch between the legs, for springs and dampers, and for a "payload" in the form of a point mass at the hip. I will explore the effect of each of these parameters on the walking cycle. The payload requires an explanatory comment: Although a useful payload certainly would *not* be a point mass at the hip, it would appear as such in the equations of motion so long as it did not rotate. That condition is reasonable; most payloads wouldn't be very useful otherwise! Again for purposes of this analysis one need not address how rotation would be prevented, although one can imagine using spring suspension, active control, or even a spin stabiliser.

3.2. Analytical Procedure

For a given parameter set, and a given slope, one would expect (at most) a single steady gait. The procedure for calculating the gait is as follows:

1. Derive linearised equations for motion during the step, and "exact" equations for the change is leg speeds at support transfer.
2. Solve the linearised equations between the start- and end-of-step.
3. Combine with the support transfer equations to get the change in state from start-of-step to start-of-step.
4. Impose the condition of cyclic repetition from step to step, and so solve for the steady gait.
5. *If* there is a solution, assess stability using step-to-step equations linearised for small perturbations on the steady cycle. (Some steady gaits are unstable!)

3.3. Equations Relating Start-of-step to End-of-step

Derivation of the equations of motion is straightforward, but sufficiently lengthy that it is best left for the appendix. The equations are simply those of a 2D open chain, with the only unusual feature being the kinematics of rolling support. The state variables are

$$\vec{\theta} = (\theta_C, \theta_F) \tag{12}$$

$$\vec{\Omega} = (\Omega_C, \Omega_F) \tag{13}$$

Note that $\theta = 0$ is by definition *normal* to the surface, and hence at angle γ to the vertical. The reference state for linearisation is resting with $\theta_C = 0$ and $\theta_F = \pi$. The linearised equations of motion then have the form

$$\mathbf{M}\,\frac{d\vec{\Omega}}{d\tau} + \mathbf{K}\Delta\vec{\theta} = \mathbf{K}\Delta\vec{\theta}_{SE} \tag{14}$$

This is a linear system in standard form; the solution for the end-of-step state is

$$\Delta\vec{\theta}(\tau_k) = \mathbf{D}_{\theta\theta}\,(\Delta\vec{\theta}_k - \Delta\vec{\theta}_{SE}) + \mathbf{D}_{\theta\Omega}\,\vec{\Omega}_k + \Delta\vec{\theta}_{SE} \tag{15}$$

$$\vec{\Omega}(\tau_k) = \mathbf{D}_{\Omega\theta}\,(\Delta\vec{\theta}_k - \Delta\vec{\theta}_{SE}) + \mathbf{D}_{\Omega\Omega}\,\vec{\Omega}_k \tag{16}$$

$\Delta\vec{\theta}_k$ and $\vec{\Omega}_k$ are the conditions at the start of the k^{th} step. The $\mathbf{D}$ matrices are functions of the period of the step, τ_k.

The machine has a position of static equilibrium at

$$\Delta\vec{\theta}_{SE} = \Delta\vec{\theta}_W + \vec{b}\gamma \tag{17}$$

$\Delta\vec{\theta}_W$ is nonzero if the mass centre of either leg is offset from the leg axis. Apart from that effect, you might expect the equilibrium position to be legs-vertical regardless of the slope. In that case $\vec{b}$ would have elements $(-1, -1)$. Actually, though, if the foot radius is nonzero, $\vec{b}_1$ has larger magnitude: The stance leg must be inclined backward to put the machine's centre of mass over the point of support. In any case, the static equilibrium is unstable unless the feet are "large", that is, with centre of curvature above the centre of mass.

3.4. Equations for Support Transfer

The two equations for support transfer emerge from the equations of motion, and so are also derived in appendix A. They simply state conservation of angular momentum about two points: of the whole system, about the point of collision, and of the trailing leg, about the hip. These equations have the form

$$\mathbf{M}^+ \vec{\Omega}_{k+1} = \mathbf{M}^- \vec{\Omega}(\tau_k) \tag{18}$$

Note that in the small-angle equations of *motion* one can neglect the variation in the inertia matrix $\mathbf{M}$ with leg angle; most of the "action" in those equations is in the state vector. In support transfer, however, the whole effect lies in the geometry, so here the inertia matrices must be evaluated exactly for the hip half-angle at contact, α_{k+1}.

Solving for the post-transfer speeds gives

$$\vec{\Omega}_{k+1} = (\mathbf{M}^+)^{-1} \mathbf{M}^- \vec{\Omega}(\tau_k) \triangleq \Lambda(\alpha_{k+1}) \vec{\Omega}(\tau_k) \tag{19}$$

3.5. Start-of-step to Start-of-step Equations

The leg angles at the start- and end-of-step are

$$\textit{start}: \quad \Delta\vec{\theta}_k = \begin{bmatrix} -1 \\ 1 \end{bmatrix} \alpha_k \tag{20}$$

$$\textit{end}: \quad \Delta\vec{\theta}(\tau_k) = \begin{bmatrix} 1 \\ -1 \end{bmatrix} \alpha_{k+1} \tag{21}$$

With these specified the step-to-step variation in α follows directly from the equations of motion (14). It must satisfy both of

$$\begin{bmatrix} 1 \\ -1 \end{bmatrix} \alpha_{k+1} = \mathbf{D}_{\theta\theta} \begin{bmatrix} -1 \\ 1 \end{bmatrix} \alpha_k + [\,\mathbf{I} - \mathbf{D}_{\theta\theta}\,]\,\Delta\vec{\theta}_{SE} + \mathbf{D}_{\theta\Omega}\,\vec{\Omega}_k \tag{22}$$

The corresponding equations for the speed vector follow from combination of (16) with the support transfer conditions (19):

$$\vec{\Omega}_{k+1} = \Lambda\,\mathbf{D}_{\Omega\theta} \begin{bmatrix} -1 \\ 1 \end{bmatrix} \alpha_k - \Lambda\,\mathbf{D}_{\Omega\theta}\,\Delta\vec{\theta}_{SE} + \Lambda\,\mathbf{D}_{\Omega\Omega}\,\vec{\Omega}_k \tag{23}$$

3.6. Solution for the Steady Gait

To solve for the steady gait, one simply imposes the conditions for cyclic repetition on the step-to-step equations:

$$\begin{aligned} \alpha_{k+1} &= \alpha_k = \alpha_0 \\ \vec{\Omega}_{k+1} &= \vec{\Omega}_k = \vec{\Omega}_0 \end{aligned} \tag{24}$$

This gives 4 equations (22, 23) in 5 parameters: (γ, τ_0, α_0, Ω_{C_o}, Ω_{F_o}). Which to choose as the independent variable? One might think of specifying γ and calculating the rest, since that's analogous to the way an experiment would be done. However, since the step-to-step equations are linear in γ (in $\Delta\vec{\theta}_{SE}$), but nonlinear in τ_0 and α_0, it is easier to specify one of the latter instead. α_0 is the more intuitively accessible, so that seems the best choice.

The derivation proceeds as follows: First, solve (23) for the speed vector $\vec{\Omega}_0$:

$$\vec{\Omega}_0 = [\,\mathbf{I} - \Lambda\,\mathbf{D}_{\Omega\Omega}\,]^{-1}\,\Lambda\,\mathbf{D}_{\Omega\theta} \left(\begin{bmatrix} -1 \\ 1 \end{bmatrix} \alpha_0 - \Delta\vec{\theta}_{SE} \right) \tag{25}$$

Then substitute into the "angle" equation (22); the end result can be written as follows. Define

$$\mathbf{D}'(\alpha_0, \tau_0) \triangleq \mathbf{D}_{\theta\theta} + \mathbf{D}_{\theta\Omega}\,[\,\mathbf{I} - \Lambda\,\mathbf{D}_{\Omega\Omega}\,]^{-1}\,\Lambda\,\mathbf{D}_{\Omega\theta} \tag{26}$$

Then

$$[\,\mathbf{D}' + \mathbf{I}\,] \begin{bmatrix} -1 \\ 1 \end{bmatrix} \alpha_0 = [\,\mathbf{D}' - \mathbf{I}\,]\,\Delta\vec{\theta}_{SE} \tag{27}$$

An equivalent form is

$$[\,\mathbf{D}' + \mathbf{I}\,] \begin{bmatrix} -1 \\ 1 \end{bmatrix} \alpha_0 - [\,\mathbf{D}' - \mathbf{I}\,]\,\Delta\vec{\theta}_W = [\,\mathbf{D}' - \mathbf{I}\,]\,\vec{b}\,\gamma \tag{28}$$

With α_0 specified, this is a pair of simultaneous equations for γ and τ_0 (in $\mathbf{D}'$). Once the solution

is found, the speed vector follows from (25), and the steady walk is fully specified.

We use Newton's method to solve (28) for τ_0. With most parameter sets a starting τ_0 of 2/3 the period of the swing leg (as suggested by (11) in the synthetic wheel analysis) leads to convergence after about 5 iterations, usually at a somewhat shorter step period. However, in some situations the iteration fails to converge, or converges to an unstable walk, when in fact a perfectly good walk is there to be found. When suspicious we search "manually" for a better starting point, which in such cases usually has to be selected very carefully.

3.7. Gait Stability Analysis

Stability for small perturbations on the walking cycle can be assessed by linearising equations (22, 23). For small perturbations on the gait, the transition matrices $\mathbf{D}_{\theta\theta}(\tau_k)$, *etc.*, and the support transfer matrix $\Lambda(\alpha_{k+1})$ can be approximated as follows:

$$\mathbf{D}_{\theta\theta}(\tau_k) \approx \mathbf{D}_{\theta\theta}(\tau_0) + \frac{d}{d\tau}\mathbf{D}_{\theta\theta}(\tau_k - \tau_0) \triangleq \mathbf{D}_{\theta\theta}(\tau_0) + \nabla\mathbf{D}_{\theta\theta}(\tau_k - \tau_0) \tag{29}$$

$$\Lambda(\alpha_{k+1}) \approx \Lambda(\alpha_0) + \frac{d}{d\alpha}\Lambda(\alpha_{k+1} - \alpha_0) \triangleq \Lambda(\alpha_0) + \nabla\Lambda(\alpha_{k+1} - \alpha_0) \tag{30}$$

After substituting these into the (22, 23) and manipulating to collect terms, one is left with the following approximate form of the step-to-step equations:

$$\begin{bmatrix} \alpha_{k+1} - \alpha_0 \\ \Omega_{C_{k+1}} - \Omega_{C_0} \\ \Omega_{F_{k+1}} - \Omega_{F_0} \\ \tau_k - \tau_0 \end{bmatrix} = \mathbf{S} \begin{bmatrix} \alpha_k - \alpha_0 \\ \Omega_{C_k} - \Omega_{C_0} \\ \Omega_{F_k} - \Omega_{F_0} \end{bmatrix} \tag{31}$$

The $\mathbf{S}$ matrix turns out to be

$$\mathbf{S} = \mathbf{S}_1^{-1}\,\mathbf{S}_2 \tag{32}$$

where $\mathbf{S}_1, \mathbf{S}_2$ in turn are as follows. Define

$$\vec{\lambda} \triangleq \begin{bmatrix} 1 \\ -1 \end{bmatrix} \tag{33}$$

Then

$$S_1 = \left[\begin{array}{c|c|c} \vec{\lambda} & \begin{matrix}0&0\\0&0\end{matrix} & \nabla D_{\theta\theta}[\vec{\lambda}\alpha_0 + \Delta\vec{\theta}_{SE}] - \nabla D_{\theta\Omega}\vec{\Omega}_0 \\ \hline \nabla\Lambda(D_{\Omega\theta}[\vec{\lambda}\alpha_0 + \Delta\vec{\theta}_{SE}] - D_{\Omega\Omega}\vec{\Omega}_0) & \begin{matrix}1&0\\0&1\end{matrix} & \Lambda(\nabla D_{\Omega\theta}[\vec{\lambda}\alpha_0 + \Delta\vec{\theta}_{SE}] - \nabla D_{\Omega\Omega}\vec{\Omega}_0) \end{array}\right] \tag{34}$$

$$S_2 = \left[\begin{array}{c|c} -D_{\theta\theta}\vec{\lambda} & D_{\theta\Omega} \\ \hline -\Lambda D_{\Omega\theta}\vec{\lambda} & \Lambda D_{\Omega\Omega} \end{array}\right] \tag{35}$$

The first three equations in (31) have the same form as an ordinary discrete-time linear system. (Note, however, that according to the fourth equation, the time between steps is specifically *not* constant.) Its eigenvalues indicate stability: If all have magnitude less than unity, then the walk is stable; the smaller the magnitude, the smaller the number of steps required to recover from a disturbance.

If the walk is stable for small perturbations, the next question to ask is about large perturbations. For example, if the machine starts toppling from its (unstable) static equilibrium (17), will it "fall" into a walk? The answer is no; actually, it will fall into the floor! Thus there is only a finite region in state space (12, 13) from which the machine will converge to the steady gait. The eigenvalues of (31) indicate the depth of the well that lies within the space, but, as I'll illustrate later, they don't indicate its breadth.

Fortunately, we have not had to study the starting problem carefully. Our test machine is started by hand; for initial experiments the technique has been to hold the legs at roughly the expected step angle, and try to start it rotating as a single unit, in the manner of a synthetic wheel. This is hardly a reliable technique, but it works often enough to be more attractive than adding self-starting capability.

4. Effect of Parameter Variations on the Walking Cycle

Our walking analysis is now complete, and ready to use for study of parameter variations. I will offer a series of examples whose collective message is that walking is a robust natural mode

of the general biped configuration. Of course an exhaustive survey of the parameter space is impossible. Even for the "basic" biped this space is four dimensional ([R, c, r_{gyr}], plus the slope γ); with all additional variables it is much larger. Nevertheless, by interpreting a series of examples one can get a clear idea of each parameter's influence. I will discuss briefly the effect of each of the following: slope, foot radius, centre of mass height, radius of gyration, hip mass, c.m. offset from the leg axis, dampers at the stance foot and the hip, and mismatch between the legs.

4.1. Scaling

Before discussing these parameter variations I should make some explicit notes on scaling. Simple addition of mass has no effect on the gait. Increasing leg length reduces the step period in proportion to $1/\sqrt{l}$, but increases the step length in proportion to l. Overall, then, the speed *increases* like $\sqrt{l}$. Varying g also has a square-root effect; thus if astronauts on the moon tried to walk as on earth, they could only travel 40% as fast. Hence, as McMahon (1984) pointed out, they hop instead.

4.2. Slope

The odd man out on the parameter list is γ, since it describes the environment rather than the machine. Figure 8 shows an example of its effect on hip half-angle α_0, dimensionless step period τ_0, and a stability index $|z|$. This last parameter is the magnitude of the largest eigenvalue of the step-to-step transition equations (31). Since this set of equations has 3 eigenvalues, the largest is only a rough measure of relative stability; however, it is the most convenient summary index. The design parameters in this example, as noted on the plot, are similar to those of our test machine. (Since the machine is the victim of constant tinkering, its parameters never remain constant for very long!)

The plot should be compared with those for our illustrative models: α_0 varies with γ in the same way as for the rimless wheel (figure 5). Meanwhile τ_0 varies as for the synthetic wheel (figure 7), which is to say, not much at all. In fact τ_0 for this example is about 0.6 of the swing

leg period, as opposed to the value of 0.65 suggested by the wheel analysis (11). Note also that since τ_0 is nearly constant, the plot of α_0 is essentially a plot of speed as well. (These trends continue to larger slopes and leg angles, but they can't be reliably calculated with linearised equations of motion.) The variation in $|z|$ must be interpreted with some care: The gait tends toward neutral stability as $\gamma \rightarrow 0$. However, this doesn't indicate a tendency for the gait to break down; rather it implies comfortable walking over a broad range of speeds, as for the synthetic wheel.

Comparison with a human is worthwhile. For me, a comfortable α_0 (measured by averaging the length of several strides) is 0.28, and the period is $0.58 sec$. With a leg length of $104 cm$, the corresponding dimensionless period is 1.8. For the same α_0 the period calculated for our test machine is 2.3, or, with a leg length of $50 cm$, $0.52 sec$. Thus in dimensionless terms the machine is slower than a human. That is partly because of fundamental differences in dynamics, but also partly by design; we chose c and r_{gyr} so things would happen as slowly as possible.

Efficiency calculations are particularly simple for gravity powered machines, since for small angles the slope is equal to the weight-specific resistance. In this example the specific resistance of walking with $\alpha_0 = 0.28$ is 0.017. Earlier I drew an analogy with aircraft; by way of continuing that comparison, 0.017 is coincidentally quite close to the specific resistance of the very best sailplane ever made. But then to keep pace with the sailplane, a passive walker would need legs $2 km$ long!

4.3. Foot Radius

The next parameter on the list is foot radius. Figure 9 shows an example. Note the slight change in format from the last figure: α_0 is constant in this example, and the three functions plotted are slope γ, period τ_0, and stability index $|z|$.

For R near unity the resistance is very small and the stability neutral, as for the synthetic wheel. As the radius decreases, the contact points at support transfer separate, and the energy lost in the collision increases. Meanwhile $|z|$ decreases, but one must be careful about interpreting this as an improvement in stability. (Incidentally, for smaller α_0 this "improvement" is even

more pronounced; $|z|$ decreases monotonically all the way to $R = 0$.) A deeper well is not always broader, as you can judge from table 2.

Table 2
Calculated range of starting speeds
from which a steady walk will be established

$\alpha = 0.3$
$R = 0.33$
$r_{gyr} = 0.32$
$c = 0.63$

R	VARIABLE	NOMINAL	MINIMUM	MAXIMUM
0.2	Ω_F	0.28	-0.15	0.44
0.2	Ω_C	0.43	0.41	0.49
0.5	Ω_F	0.34	-0.10	0.53
0.5	Ω_C	0.41	0.38	0.47

Note that these values apply with only *one* of the speeds perturbed from nominal at a time.

Table 2 was calculated using the step-to-step equations (22, 23). The calculations also indicate that convergence to the steady cycle is rapid from anywhere within the boundaries. As you can see, even with the larger feet the tolerances on initial Ω_C are strict. This explains the hit-and-miss record of our experimental starting technique. However, we preferred to live with this problem rather than make the feet large, although in future we will make R somewhat larger than 1/3. The physical reason for the sensitivity to Ω_C is that the stance leg is an inverted pendulum: the smaller the foot radius, the stronger the tendency to diverge. The stronger the tendency to diverge, in turn, the more sensitive the swing period to initial speed.

Foot radius is perhaps a peculiar measure of size; it can, however, be related to the length of a human foot. The relationship is determined by the movement of the support point between the start- and end-of-step:

$$\Delta y = 2\,\alpha_0\,R \tag{36}$$

A human foot is about 1/3 the leg length, so with a comfortable α_0 of 0.3, the "equivalent radius" is about 0.5. Hence the test machine's feet are a bit small by human standards. Of course, human

feet are not cylindrical, but I suspect that this isn't a significant difference as far as dynamics are concerned. The important feature seems to be movement of the support point during the step, so a flatter curve or even a flat foot of equivalent length probably wouldn't change the walk very much. A still more intriguing possibility is leaf-spring feet, which would make support transfer elastic, and therefore more efficient.

4.4. Centre of Mass

Figure 10 shows an example of gait variation with centre of mass position. First consider the energetics with reference to the rimless wheel: Other things being equal, the energy lost on support transfer increases with the angle between the two support points and the mass centre. This accounts for the increase in specific resistance as the mass centre descends. At some point the lost energy can't be recovered simply by moving downhill, so the gait becomes unstable. Note, however, that this lower limit on the *leg's* mass centre can be extended all the way to the foot by adding sufficient *hip* mass, which raises the *overall* mass centre. Incidentally, the kinks in the plot of $|z|$ appear because I have plotted only the largest of the three step-to-step eigenvalues (31). A kink indicates a switch in their ordering.

I've discussed the kink and instability at the low-c end; at the other extreme the problem is with the swing leg. If the inertia is held constant, then the natural period of the swing leg increases with ascending mass centre. The synthetic wheel model predicts that there should be a corresponding increase in the step period, and indeed that is indicated by the plot. But at some point the swing leg can't come forward fast enough to break the fall of the stance leg, so again the walk becomes unstable.

For the test machine c is about 0.63. We would have preferred higher for slower steps and lower resistance, but that would have required adding yet more lead ballast to the machine.

4.5. Radius of Gyration

Varying radius of gyration has effects comparable to those of moving the mass centre. These are plotted in figure 11. The variations in resistance and period are consistent with intuition; the stability presumably follows by the arguments given in the preceding section. The insta-

bility for large r_{gyr} was a constraint for us. With retraction mechanisms at one end, and a crossbar at the other, the "outer" leg pair (figure 2) without ballast has r_{gyr} near the "dumbell" limit of 0.5. To reduce r_{gyr} to an acceptable level, we had to concentrate lead at the legs' mass centre. Once the outer legs were adjusted, the centre leg was ballasted to match. The end result is that over 40% of the machine's mass is lead -- not an optimal design, but certainly a flexible one!

4.6. Hip Mass

As I mentioned in §4.4, machines with otherwise unacceptable values for c and r_{gyr} could be made stable by adding sufficient hip mass. However, if one starts with acceptable parameters, then adding hip mass doesn't have much effect at all. Figure 12 shows moderate reductions in specific resistance and speed, as one would expect with elevation of the overall mass centre. Notice that in the limit $m_{HIP} \rightarrow 1$, the "synthetic wheel approximation" holds, that is, the swing motion doesn't affect the stance motion. In this case the "synthetic wheel" has $R<1$, which makes the walk convergent rather than neutrally stable.

The important message of figure 12 is that a passive walker has a large payload capability. We haven't explored this feature, since, as I mentioned earlier, it would have required design of some mechanism for keeping the payload upright.

4.7. Offset of the Mass Centre from the Leg Axis

In the "basic" biped, the mass centre of each leg is on the axis between the hip and the foot's centre of curvature. However, the equations of motion allow for a lateral offset, and some sample calculations suggest that the dynamics are quite unforgiving of variations. With the parameters of the test machine, a stable walk is possible only for $-0.009<w<+0.002$. Actually we didn't consider lateral offset at all in assembling the test machine, and in fact the two legs came out with different values. For the outer legs w is +0.008; for the centre, -0.01. While neither value is within the stable region, it turns out to be helpful that they have opposite sign (which is the more symmetric arrangement when viewed from the side). Calculations with the step-to-step equations (22, 23) indicate that, with our example parameters, offsets of up to about

0.03 are tolerable provided they are opposite and nearly equal for the two legs. The gait varies from step to step as support alternates between the legs, but there is a steady cycle repeating over two steps. Table 3 lists some calculated results for the experimental machine.

Table 3
Steady walk calculated for the test machine

$\gamma = 0.019$
$R = 0.33$
$r_{gyr} = 0.32$
$c = 0.63$

STANCE LEG	STANCE LEG w	INITIAL α	STEP PERIOD τ_0	AVERAGE SPEED [m/s]
outer	+0.008	0.244	2.35	0.51
centre	-0.01	0.281	2.51	0.48

4.8. Damping

Damping of the moving parts is undesirable. However, it is also unavoidable, so its effect warrants some study. The main sources of damping are friction on the stance foot and in the hip bearings. According to common friction models, the damping might be coulombic (*i.e.* a constant torque opposing the motion) or linear (*i.e.* an opposing torque proportional to speed). Our interest is in getting a rough idea of the effect of dissipation, rather than worrying about the details of how it arises; hence I will use the model which is more simply accommodated within the equations of motion.

Coulomb friction can be represented by adding a constant vector to the RHS of (14). In the case of friction on the stance foot, the effect is similar to offsetting the stance leg's *c.m.* backward ($w < 0$). Coulomb friction on the hip is harder to handle, because the angular speed at the joint reverses during the step; hence (14) would have to be solved piecewise.

Viscous friction, on the other hand, is easy to treat; one need only introduce a damping matrix **F** into (14):

$$\mathbf{M}\,\frac{d\vec{\Omega}}{d\tau} + \mathbf{F}\,\vec{\Omega} + \mathbf{K}\Delta\vec{\theta} = \mathbf{K}\Delta\vec{\theta}_{SE} \tag{37}$$

For a damper at the hip, **F** is

$$\mathbf{F} = \begin{bmatrix} f & -f \\ -f & f \end{bmatrix} \tag{38}$$

For a damper at the stance foot, all elements are zero except F_{11}. Note that f is non-dimensionalised by $m\sqrt{gl^3}$.

Table 4 lists some sample results. They indicate that quite strong damping on the stance foot can be balanced by increasing the slope. On the other hand, only a little damping at the hip joint sabotages the steady walk. Thus if a hip damper is suddenly turned on the walk will decay, although the decay can extend over many steps if f is close to the limit for a steady solution.

Table 4
Maximum damping coefficients
with which passive walking will remain stable

$\alpha = 0.3$
$r_{gyr} = 0.32$
$c = 0.63$

DAMPED JOINT	FOOT RADIUS	VISCOUS DAMPING COEFFICIENT	SLOPE	EIGENVALUES SWING MODE	EIGENVALUES TOPPLING MODE
stance foot	0.33	0.18	0.078	-0.042 ± 1.47*i*	+0.72 -1.03
stance foot	0.5	1.05	0.255	-0.138 ± 1.35*i*	+0.25 -2.24
hip	0.33	0.0017	0.031	-0.007 ± 1.48*i*	±0.859
hip	0.5	0.0052	0.027	-0.022 ± 1.51*i*	+0.677 -0.680

Our machine has 1/4 inch ball bearings, whose friction we've observed during the course of adjusting leg parameters. That is, to determine each leg's radius of gyration, we time pendulum swings over several tens of cycles, while keeping the other leg clamped. f of 0.0017 would cause a 3% reduction in amplitude per cycle. The observed decay is comparable but probably smaller. (We haven't checked carefully.) Thus the bearing friction is marginally acceptable with R of 1/3, and would certainly be adequate with a larger R. (On this point it is worth noting that the amplitude of these test swings is about half that experienced in a comfortable walk.

Therefore if the damping is coulombic rather than linear, the "effective" f during walking is less than the pendulum test suggests.)

4.9. Leg Mismatch

The centre leg and outer pair of the test machine have been ballasted to match within the following limits:

$$|\Delta m| < 10^{-2}$$
$$|\Delta c| < 2 \times 10^{-3}$$
$$|\Delta r_{gyr}| < 4 \times 10^{-3}$$
$$|\Delta l| < 5 \times 10^{-3}$$

One would certainly hope that this level of mismatch is not a problem, but since a calculation is straightforward we have checked by solving the equations of motion (22, 23) over several steps. Figure 13 shows the leg trajectories for an example with legs matched except for a 10% difference in mass. You can see the similarity between the motion of this machine and that of the ideal synthetic wheel (figure 7). However, here the cycle repeats over not one, nor two, but rather four steps. Of course there would be a one-step cycle with no mismatch, and a two-step cycle with only a small mismatch. Here, then, is an example of frequency jumping, which is not uncommon among nonlinear systems. But aside from this curiousity, the main point is that the dynamics are tolerant of mismatch between the legs.

5. Experiments

6. The Test Machine

Having run through the general effects of each design variable, we now turn to the specific example of our test machine. To expand on the description already given, its mass is primarily aluminum structure and lead ballast. The feet are 1/16 aluminum strips, 1 inch wide, and subtending an arc of $0.75 rad$. These are soled with rubber matting. Membrane switches are glued inside the sole on the rear part of each foot. Closing of any of these switches triggers lifting of the feet on the opposite leg, followed by re-extention in time for support transfer. The throw is $16 mm$, and the sequence takes $0.5 sec$. The feet are lifted by DC motors driving jackscrews.

Power for the motors is supplied by 6 Ni-Cad "AA" cells, and for the sequencing electronics by an independent set of 4 "AA" cells. Each motor weighs only about $50gm$ and is far too weak to move the whole machine. It would be particularly appropriate to describe the jackscrew mechanism as an Achilles' heel. Our best test to date has produced only 4 support transfers in series before one of these failed. So we are anxiously redesigning the mechanism, but in the meanwhile we can make some comments on results thus far.

6.1. Experimental Results

Figure 14 shows a series of steps, in the form of hip angle *vs* time. Hip angle is defined as positive if the centre leg is ahead of the outer leg, so in steady walking it would be cyclic over two steps. The method for making the measurement warrants a brief comment. The machine itself does not have angle sensors. Instead, we used frame-by-frame photogrammetry of VHS tape. Each frame shows a perspective projection of the machine. We inverted the projection by a least-squares estimation technique similar to one described by Tsai (1987). There is a gap near the beginning of the record; in this interval a poor viewing angle, combined with rather blurry video, prevented accurate measurement. Otherwise checks of the photogrammetry technique against test cases gives us high confidence in the hip angle estimates. (Of course we would have preferred to measure the individual leg angles rather than their difference, but when the tape was made we hadn't thought to include the necessary vertical reference in the image.)

This trial was done on a tabletop inclined at $0.019rad$, and the expected gait on this slope was given in table 3. Our manual starting technique left the machine with a initial hip angle rather larger than the steady-cycle amplitude. Consequently the motion of the swing leg was slightly exaggerated during the first step, and the period relatively long. The next two steps indicate a relatively steady motion, which continued into the fourth step. The centre foot then retracted on cue, but didn't re-extend, so the machine had an experience similar to a human encountering an unexpected step down.

Table 5 lists the periods and lengths of the steps. One would not expect these to agree precisely with the calculated steady cycle, as given in table 3, since these initial steps must include some perturbations due to the starting transient. However, that turns out to be insufficient to

explain the discrepancies. The measured amplitude is roughly 10% larger, and the period roughly 10% longer, than the model predicts.

Table 5
Parameters of the steps plotted in figure 14

STEP	SUPPORT LEG	INITIAL α	PERIOD [sec]	τ
1	centre	0.34	0.68	2.9
2	outer	0.28	0.62	2.65
3	centre	0.31	0.63	2.7
4	outer	0.28	-	-

The discrepancy may arise in the equations for motion during the step (14) or for support transfer (19). The equations of motion are more easily checked. We measure parameters of each leg as follows: mass with an ordinary balance; c with a knife edge; r_{gyr} by pendulum oscillation with the opposite leg clamped; and R and w most reliably by finding equilibrium angles ($\Delta\vec{\theta}_{SE}$ in (17)) $vs\,\gamma$. These parameters are inserted into the equations of motion (14), and 4 eigenvalues and eigenvectors emerge. Two are real, corresponding to the toppling mode, and two are imaginary, corresponding to the swing leg's pendulum motion.

According to the synthetic wheel model, the swing mode is the most important factor in determining the step period (11). The question is whether this mode is correctly predicted by the equations of motion, given the parameters measured as described above. One can check as follows: Stand the machine on a flat surface, set the leg angles in the ratio specified by the swing-mode eigenvector, and release. Ideally a persistent oscillation in the swing mode should ensue. Of course, since the machine also has an unstable mode, this experiment is in practice very brief. However, we've found it fairly easy to get at least two clear swing-mode oscillations before toppling develops; these provide sufficient data for our purposes. Again using a video camera as the measuring device, we have found a swing-mode period of $0.98 \pm 0.01 sec$ with the stance leg rolling, as opposed to $1.17 sec$ with the stance leg clamped. This result agrees with the prediction.

Despite agreement on this most important point, there may be some smaller discrepancies in the equations of motion due to non-ideal behaviour of the feet. While measuring static

equilibria *vs* slope, we were surprised to find that on some slopes the equilibrium was stable, albeit for quite small perturbations. Evidently the feet flatten locally, despite behaving over larger displacements as cylinders with $R=1/3$.

In view of the agreement between measured and calculated swing periods, however, we are most inclined to suspect support transfer as the primary agent of discrepancy. On this point it is worth reviewing (11), according to which one step of the synthetic wheel requires about 2/3 of the swing period (*i.e.* $\omega_F \tau_0 = 4.06$). For the test machine, the prediction is $\omega_F \tau_0 \approx 3.6$; the measurement is $\omega_F \tau_0 \approx 4.0$. So we are seeing behaviour which is closer than expected to that of the synthetic wheel, and this may be due to higher-than-expected efficiency in support transfer. That, in turn, would arise if the feet had some spring action. Of course 1/16 inch aluminum strip is in this context rather flexible, so elastic effects are certainly conceivable.

From a modeller's point of view elasticity is a complication, but as far as efficiency is concerned, it is all to the good. In any event, we will make improvements in the feet before studying support transfer in detail. For now the experimental results indicate that the machine behaves approximately as the model predicts. Thus one can have some confidence that the conditions specified by the model can be realised in practice.

7. Improvements to Passive Walking

We have now discussed the physics, mathematics, and experimental demonstration of passive walking. The balance of the paper is devoted to some comments on exploiting the dynamics in a useful walking machine. Required abilities include steering, climbing shallow and steep slopes, and varying the stride from step to step to hit irregular footholds. But before taking up these issues, consider first the problem of passive foot clearance.

7.1. Fully Passive Walking

Since our test machine is for model verification rather than practical use, active foot clearance is actually desirable: It allows us to keep the dynamics as simple as possible. However, the toy of figure 1 is fully passive, and it would be nice to do the same in a practical machine.

One could argue that this is just an aesthetic concern, since both the control and energy required for foot clearance should be incidental. In practice, though, foot clearance can be expensive. Our machine, weighing $4kg$ and having a typical specific resistance of about 0.02, has a "fundamental" energy dissipation of about $0.2J$ per step. On the other hand, each foot actuator, moving only about $80gm$, consumes about $3J$ per step! The energy is more or less equally divided between heating the electronics, the motor, and the jackscrew mechanism; an entirely negligble fraction actually goes into motion of the foot. Presumably the drives could be improved; however, since it apparently isn't completely trivial to reach fundamental limits with an active mechanism, perhaps a passive solution would be more attractive.

7.1.1. Lateral Rocking

The toy of figure 1 clears its feet by lateral rocking. Again the dynamics are most easily illustrated by considering the synthetic wheel. The toy's feet are circular in fore/aft section, as are those of the synthetic wheel of figure 6. But a close look at figure 1 will reveal that together the feet also form a circular arc in lateral section. The centre of lateral curvature is *above* the overall mass centre, which makes side-to-side rocking a pendulum-like oscillation. In walking this oscillation should proceed in phase with each step, and with the frequency tuned so that one step takes one-half the rocking period. Thus from (11), the swing and lateral rocking frequencies should be in the ratio

$$\frac{\omega_F}{\omega_{LR}} = \frac{4.058}{\pi} \tag{39}$$

If this condition is satisfied, then walking is lossless, as for the 2D wheel. (There is an additional requirement that the oscillations be phase-locked. As it turns out, support transfer "automatically" eliminates an initial phase error over several steps.) If the tuning condition is not satisfied, then there is an energy loss on each step; if the mistuning is too large, then there is no walk at all.

Regardless of the frequency ratio, however, this "3D" synthetic wheel model requires that the feet have *zero* lateral separation. In practice one might prefer wider separation for better lateral stiffness. This becomes problematic, as one can appreciate by rocking a VHS cassette, for

example: The motion is more long-lived with support on the short rather than the long side. Incidentally, an analysis of this motion is presented by McGeer (1988); it is an example for which the impulsive treatment of support transfer is very accurate. For our purposes, though, the point is that the wider the foot spacing, the greater the energy lost on each rock. This must be recovered from the forward motion, but it turns out that only a small amount of energy can be transferred on each step. Hence a walk can be sustained only with narrow foot spacing.

Actually in our analysis of this sort of 3D walking (which is analogous to that presented in this paper) we have neglected yaw, that is, rotation about the vertical axis. Yaw does improve transfer of energy from forward motion to rocking. However, the fact remains that the toy of figure 1, and its quadruped counterpart, have quite narrow foot spacing. Moreover, their pure-rocking motion is relatively persistent, so they are certainly designed to minimise energy loss.

7.1.2. Passive Foot Clearance without Rocking

The problems of tuning (39) and lateral stiffness make rocking unattractive, but presumably there are other schemes for fully passive walking. Thoughts on how to do it *without* using the third dimension have led me to consider a modification of the stiff-legged walker which is remarkably anthropomorphic (figure 15). Clearance during the swing phase is arranged by flexing the leg at the knee. During the stance phase, the knee is prevented from rotating by a mechanical stop. The arc of the foot must be abbreviated on the "heel" side to ensure that the support force holds the knee to the stop during the initial part of stance.

When the support force is removed at the start of the swing phase, a spring launches the lower leg on a ballistic trajectory. It seems preferable to use the spring only to provide a starting impulse, rather than to drive the whole trajectory, since the swing period will then be relatively insensitive to variations in spring stiffness. In any case, the period must be tuned so that the lower leg is repositioned in time to catch the next support transfer. Again positioning is not absolutely critical; the knee only need be within a range such that the impact locks it.

Incidentally, by the same qualitative discussion one could argue that such a design could walk in either direction, just as a human can walk forwards and backwards. At present, however, the argument is purely qualitative, and some analysis is required to establish whether these legs

really could walk passively.

7.2. Steering

Steering is related to the foot clearance problem. Our test machine doesn't even have a *dimension* for steering, let alone a mechanism. A steerable version is possible, just as it is possible for one to steer when walking on crutches. Steering would be easier, however, with a true biped. That would make support point-like and so offer little resistance to rotation about the vertical axis. One could steer by applying a torque at the hip, or, perhaps, by biasing the walking cycle with small adjustments in leg length.

Of course the key problem with a true biped is sideways toppling. A machine whose left and right legs were confined to parallel fore/aft planes obviously wouldn't work; it would fall sideways as soon as one leg left the ground. Instead each leg during its support phase must rotate inward under the overall mass centre. A line of human footprints provides a simple demonstration: footfalls have much smaller lateral spacing than the width of the hip would suggest. It remains to be seen whether such a lateral cycling of the legs could be combined with 2D passive walking. If there could be a passive cycle, it seems that it would have to be actively stabilised to prevent sideways toppling. Since this active input would only counter disturbances, however, it would not necessarily be a large burden on the controller or the power supply. (Although the lesson of our foot retraction scheme indicates that efficient implementaion might not be trivial!)

7.3. Powered Walking

As we suggested in the introduction, hill climbing and step-to-step stride variation can be achieved by a fairly simple extention of the passive walking model. Options for energy input are torquing at the hip and impulsively pushing-off at the end of stance. The latter is analogous to flexing of the ankle in a human walk, and is tidier analytically. It would enter the walking equations at the same point as the support transfer condition (19), and so modify the step-to-step equations (22, 23). Solutions for the steady cycle and step-to-step stability would follow as before, with the magnitude and direction of the impulse as additional design parameters. Options for physical implementation include stronger versions of our current jackscrew drives, or

spring-loaded pistons which would be cocked during swing phase.

7.4. Gait Variation

Once one has such a physical capacity for energy input, one also has an effective means for control of the stride. Our fundamental concept is that control should involve only a small perturbation on the passively generated cycle, and this concept has a precise analytical expression. One can formulate the linearised step-to-step equations (31) with the push-off impulse as the control variable. One can then choose control laws using standard methods for discrete-time linear systems.

The control law would require both feedback and feedforward components. The feedback component would maintain a specified stride (*i.e.* α_0) despite, for example, variations in slope while traversing rolling terrain. It would require several strides to recover from a change in slope or other disturbance. Feedforward would handle situations requiring faster response, such as hitting a foothold selected only one step in advance. (Feedforward implies using the step-to-step equations of motion to calculate the required push-off impulse. Consequently the technique is sensitive to parameter errors, but there is no alternative if one needs such fast action. Feedback control is more robust, but slower.)

In some situations foothold specification one step in advance may be too much to ask; an adjustment may be necessary during the final step itself. Such an adjustment would require a new actuator as well as additions to the control law. Applying torque at the hip is one option. Alternatively, following the human example, one could use ankle motion to move the support point longitudinally along the foot, which varies the torque on the machine.

7.5. Steep Slopes

Passive walking with fixed leg lengths cannot be sustained on slopes exceeding a few degrees; the collision at support transfer isn't sufficient to dissipate the kinetic energy accumulated during the step. Descending a steep slope such as a staircase would require some compression of the leg, both for energy dissipation and simply to hit the footholds with reasonable leg angles. Analogous requirements apply for climbing. We hope to find that the changes in leg

lengths can be sufficiently "decoupled" from the pendulum motion that longitudinal positioning can still proceed passively.

8. Summary

The analytical model for the biped of figure 3 indicates the simplicity and efficiency of passive walking, and its robustness with respect to most design variables. Preliminary results with the experimental machine, figures 2 and 14, demonstrate that the model can be implemented in practice. Our comments in these last few pages describe how the dynamics of passive walking may be expected to generalise beyond our two-dimensional, unpowered, stiff-legged, and circular-footed demonstrator, and so be applied to practically useful machines. Efficiency and ease of control are the attractions relative to systems requiring active gait generation. Some care is required to realise these advantages, particularly to ensure low hip damping, and more experimental and analytical work is required to see how far the passive walking principle can be extended. However, the promise of getting something for nothing is well worth pursuing.

9. Appendix

9.1. Dynamics of an *N*-link Chain with Rolling Support

We will now derive the linearised equations of motion (14). Although we are interested in a machine with only 2 links, there is little extra effort in deriving general equations for an *N*-link, two-dimensional, open chain. Figures 16 and 17 illustrate the necessary notation.

The dynamics can be expressed in N second-order equations, each of which has the form

$$\frac{dH_n}{dt} = T_n \qquad \text{(A1)}$$

where T_n is the torque applied to the n^{th} joint, and H_n is the angular momentum of links n through N about the instantaneous position of the n^{th} joint. In the case of n=1, this position is the point of contact between the foot and the ground.

(A1) is the most obvious basis for deriving the dynamics, but formulation is actually easier if one uses the form

$$\frac{d}{dt}(H_n - H_{n+1}) = T_n - T_{n+1} \qquad \text{(A2)}$$

The objective is to express these equations in terms of the angular rates Ω_1 through Ω_N. H_n is

$$H_n = \sum_{p=n}^{N} J_p \, \Omega_p + \sum_{p=n}^{N} m_p \, (\vec{r}_{np} \times \vec{V}_p) \tag{A3}$$

Therefore

$$H_n - H_{n+1} = J_n \, \Omega_n + m_n \, \vec{r}_{nn} \times \vec{V}_n + \sum_{p=n+1}^{N} m_p \, (\vec{r}_{np} - \vec{r}_{n+1,p}) \times \vec{V}_p \tag{A4}$$

Some care must be exercised in calculating the derivative of this expression, as required by (A2). Bear in mind that H_n is taken with respect to a fixed point in space, which is occupied by joint n only instantaneously. Thus the position vectors are treated as constants in the differentiation, which is therefore simply

$$\frac{d}{dt}(H_n - H_{n+1}) = J_n \frac{d\Omega_n}{dt} + m_n \, \vec{r}_{nn} \times \frac{d\vec{V}_n}{dt} + \sum_{p=n+1}^{N} m_p \, (\vec{r}_{np} - \vec{r}_{n+1,p}) \times \frac{d\vec{V}_p}{dt} \tag{A5}$$

From figure 16 and 17, the position vectors are as follows:

$$\begin{aligned} \vec{r}_{nn} &= c_n \hat{x}_n + w_n \hat{y}_n \qquad n = 2, 3, \ldots, N \\ \vec{r}_{11} &= c_1 \hat{x}_1 + w_1 \hat{y}_1 + R(\hat{x} - \hat{x}_1) \end{aligned} \tag{A6}$$

$$\begin{aligned} \vec{r}_{np} - \vec{r}_{n+1,p} &= l_n \hat{x}_n \qquad n = 2, 3, \ldots, N \\ \vec{r}_{1p} - \vec{r}_{2p} &= l_1 \hat{x}_1 + R(\hat{x} - \hat{x}_1) \end{aligned} \tag{A7}$$

Meanwhile, the kinematics of the chain require that the velocities satisfy

$$\vec{V}_n - (c_n \hat{y}_n - w_n \hat{x}_n) \Omega_n = \vec{V}_{n-1} + (d_{n-1} \hat{y}_{n-1} + w_{n-1} \hat{x}_{n-1}) \Omega_{n-1} \qquad n = 2, 3, \ldots, N$$

$$\vec{V}_1 = (c_1 \hat{y}_1 - w_1 \hat{x}_1 + R(\hat{y} - \hat{y}_1)) \Omega_1 \tag{A8}$$

Solving these for $\vec{V}_n$ in terms of the angular rates leaves

$$\vec{V}_n = (c_n \hat{y}_n - w_n \hat{x}_n) \Omega_n + \sum_{p=1}^{n-1} l_p \hat{y}_p \Omega_p + R(\hat{y} - \hat{y}_1) \Omega_1 \tag{A9}$$

The acceleration is therefore

$$\frac{d\vec{V}_n}{dt} = (c_n \hat{y}_n - w_n \hat{x}_n)\frac{d\Omega_n}{dt} + \sum_{p=1}^{n-1} l_p \hat{y}_p \frac{d\Omega_p}{dt} + R(\hat{y} - \hat{y}_1)\frac{d\Omega_1}{dt} -$$

$$(c_n \hat{x}_n + w_n \hat{y}_n)\Omega_n^2 - \sum_{p=1}^{n-1} l_p \hat{x}_p \Omega_p^2 + R \hat{x}_1 \Omega_1^2 \qquad \text{(A10)}$$

More simply, this expression has the form

$$\frac{dV_{n_x}}{dt} = \sum_{p=1}^{N} X_{np} \frac{d\Omega_p}{dt} + \sum_{p=1}^{N} A_{np} \Omega_p^2$$

$$\frac{dV_{n_y}}{dt} = \sum_{p=1}^{N} Y_{np} \frac{d\Omega_p}{dt} + \sum_{p=1}^{N} B_{np} \Omega_p^2 \qquad \text{(A11)}$$

Substituting these formulas and the position vectors (A6, 7) into (A5) produces an expression of the form

$$\frac{d}{dt}(H_n - H_{n+1}) = = \sum_{p=1}^{N} M_{np} \frac{d\Omega_p}{dt} + \sum_{p=1}^{N} C_{np} \Omega_p^2 \qquad \text{(A12)}$$

Each coefficient M_{np} and C_{np} varies with the joint angles, through the various cross products in (A5). In fact for stance dynamics *linearised* with respect to zero angular speed, the coefficients C_{np}, and hence A_{np}, B_{np} in (A11), are not used and need not be calculated. We do the remaining calculations in *APL*, as follows:

1. One routine calculates $(\sin\theta_n, \cos\theta_n)$, $n = 1, N$.
2. Using these results and the dimensions of the links, the next routine calculates the $2N^2$ coefficients X, Y in (A11).
3. Using these results and the link masses and inertias, the next routine calculates the N^2 coefficients M in (A12) using (A5, 6, 7).

Now according to (A2) and (A12), the n^{th} equation of motion is

$$\sum_{p=1}^{N} M_{np} \frac{d\Omega_p}{dt} + \sum_{p=1}^{N} C_{np} \Omega_p^2 = T_n - T_{n+1} \qquad \text{(A13)}$$

For the *RHS* we need the torque. The principle torque is due to gravity, and can be expressed as follows:

$$T_{g_n} = \sum_{p=n}^{N} m_p (\vec{r}_{np} \times \vec{g}) \qquad \text{(A14)}$$

Taking the difference required by (A2), then, produces

$$T_{g_n} - T_{g_{n+1}} = m_n \vec{r}_{nn} \times \vec{g} + \sum_{p=n+1}^{N} m_p (\vec{r}_{np} - \vec{r}_{n+1,p}) \times \vec{g} \qquad \text{(A15)}$$

In scalar terms, the expression is

$$T_{g_n} - T_{g_{n+1}} = g \left[\left[\left(m_n c_n + \left(\sum_{p=n+1}^{N} m_p \right) l_n \right) \sin(\theta_n + \gamma) + m_n w_n \cos(\theta_n + \gamma) \right] \right]$$
$$n = 2, 3, \ldots, N$$

$$T_{g_1} - T_{g_2} = g \left(\sum_{p=1}^{N} m_p \right) R \sin\gamma +$$
$$g \left[\left[\left(m_1 (c_1 - R) + \left(\sum_{p=2}^{N} m_p \right) (l_1 - R) \right) \sin(\theta_1 + \gamma) + m_1 w_1 \cos(\theta_1 + \gamma) \right] \right] \quad \text{(A16)}$$

This is linearised about the vertical, *i.e.* $\gamma = 0$ and $\theta_n = 0$ *or* π. (For the biped (14) in particular, $\theta_1 = 0, \theta_2 = \pi$.) Thus

$$T_{g_n} - T_{g_{n+1}} \approx g \left[\pm m_n w_n + \left[m_n c_n + \left(\sum_{p=n+1}^{N} m_p \right) l_n \right] \right] (\theta_n + \gamma)$$
$$n = 2, 3, \ldots, N$$

$$T_{g_1} - T_{g_2} \approx g \left[\pm m_1 w_1 + \left[m_1 (c_1 - R) + \left(\sum_{p=2}^{N} m_p \right) (l_1 - R) \right] \right] \theta_1 +$$
$$g \left[m_1 c_1 + \left(\sum_{p=2}^{N} m_p \right) l_1 \right] \gamma \quad \text{(A17)}$$

The "+" applies for $\theta_{n_0} = 0$; "-" for $\theta_{n_0} = \pi$. Additional torque terms can also be added to this expression, such as we have done to calculate the effect of damping in §4.8.

Including only the gravitational torque, however, the linearised equation of motion for link n, from (A15), is

$$\sum_{p=1}^{N} M_{np} \frac{d\Omega_p}{dt} = T_{g_n} - T_{g_{n+1}} \quad \text{(A18)}$$

Thus the coefficients in (A12) are all one needs to formulate the LHS. Combining all N equations in a matrix form produces (14).

9.2. Support transfer

Bookeeping for support transfer requires

1. rotating each link's unit vectors by π
2. changing the sign of w_n
3. exchanging c_n and d_n
4. reversing the order of link indices, since link 1 is always the contact link.

It also entails a change in each link's angular velocities. We approximate support transfer as an instantaneous event. This implies that contact produces impulsive *forces* at each joint. However, there are no impulsive *torques*. Consequently, H_n (as defined with the post-transfer link indexing) is conserved in support transfer. That is

$$\sum_{p=1}^{N} M_{np}^{+} \Omega_p^{+} = \sum_{p=1}^{N} M_{np}^{-} \Omega_p^{-} \qquad \text{(A19)}$$

(18) combines N of these equations in matrix form.

M_{np}^{+} is evaluated, as in (A12), using the *post*-transfer link parameters and velocities. Thus it can be calculated using the procedure outlined in §9.1. M_{np}^{-}, on the other hand, must be evaluated with the *post*-transfer link parameters, but the *pre*-transfer velocities. Thus a slightly different procedure applies:

1. Calculate the $2N^2$ coefficients X_{np}, Y_{np} using *pre*-transfer link parameters.
2. Renumber *both* sets of indices, *i.e.* $X_{np} \rightarrow X_{N-n,N-p}$, *etc.*
3. With these coefficients and the *post*-transfer link parameters, find the N^2 coefficients M_{np}^{-} according to (A4).

Thus we use the same set of routines as for evaluating (A12) in the dynamics analysis, and simply modify the input data.

References

McGeer, T. 1988. Wobbling, Toppling, and Forces of Contact. Submitted to *The American Journal of Physics*, April 1988.

McMahon, T.A. 1984. Mechanics of locomotion. *Int. J. Robotics Res.* Vol.3(2)

Mita, T. et al. 1984. Realisation of a high speed biped using modern control theory. *Int. J. Control* Vol.40(1).

Miura, H., Shimoyama, I., 1984. Dynamic walking of a biped. *Int. J. Robotics Res.* Vol.3(2).

Raibert, M.H. 1986. Legged robots the balance. MIT press.

Russell, M. 1983. Odex 1: The first functionoid. *Robotics Age* 5:12-18.

Tsai, R.Y., 1987. A versatile camera calibration technique for high-accuracy 3D machine vision metrology using off-the-shelf TV cameras and lenses. *IEEE J. Robotics and Automation.* Vol.RA-3(4).

Waldron, K.A., 1986. Force and motion management in legged locomotion. *IEEE J. Robotics and Automation.* Vol.2(4).

Yamada, M., Furusho, J., and Sano, A. 1985. Dynamic control of a walking robot with kick action. *Proc. Int. Conf. on Advanced Robotics.*

Figure 1 *A bipedal toy which walks passively down shallow inclines. The dynamics of wobbling are similar.*

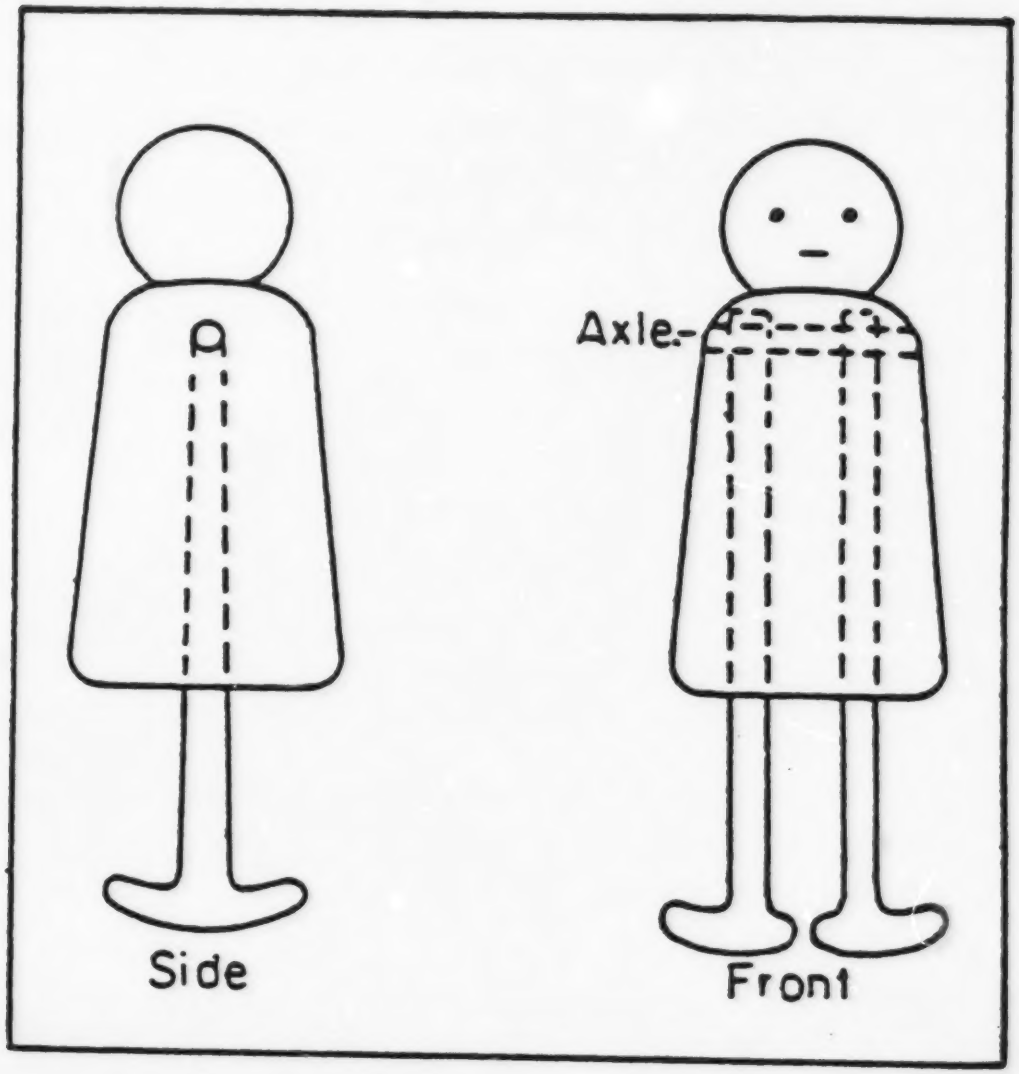

Figure 2. *The experimental machine, a "two-dimensional" version of the walking toy. The legs are about one-half human scale.*

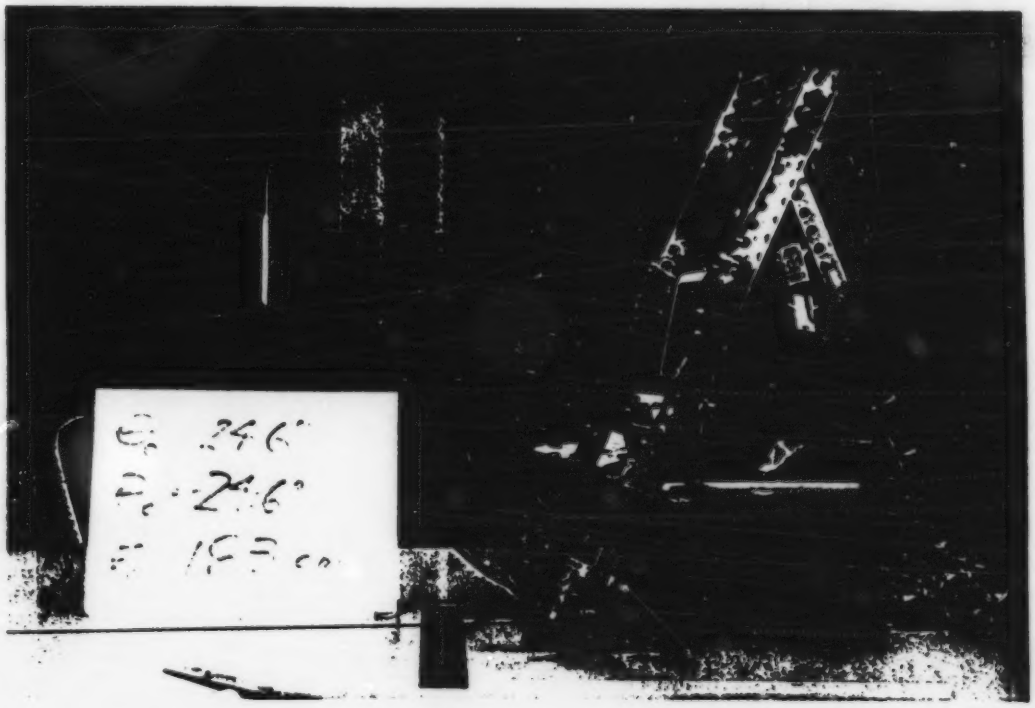

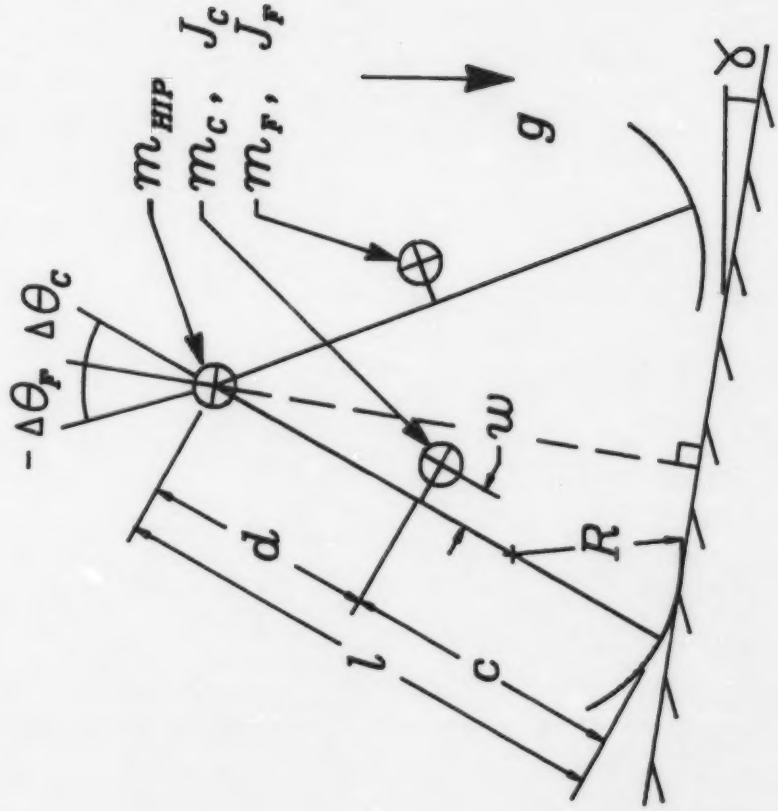

Figure 3. *General configuration of a two-dimensional biped.*

Figure 4. *A "rimless wheel," which once started settles into a steady downhill walk.*

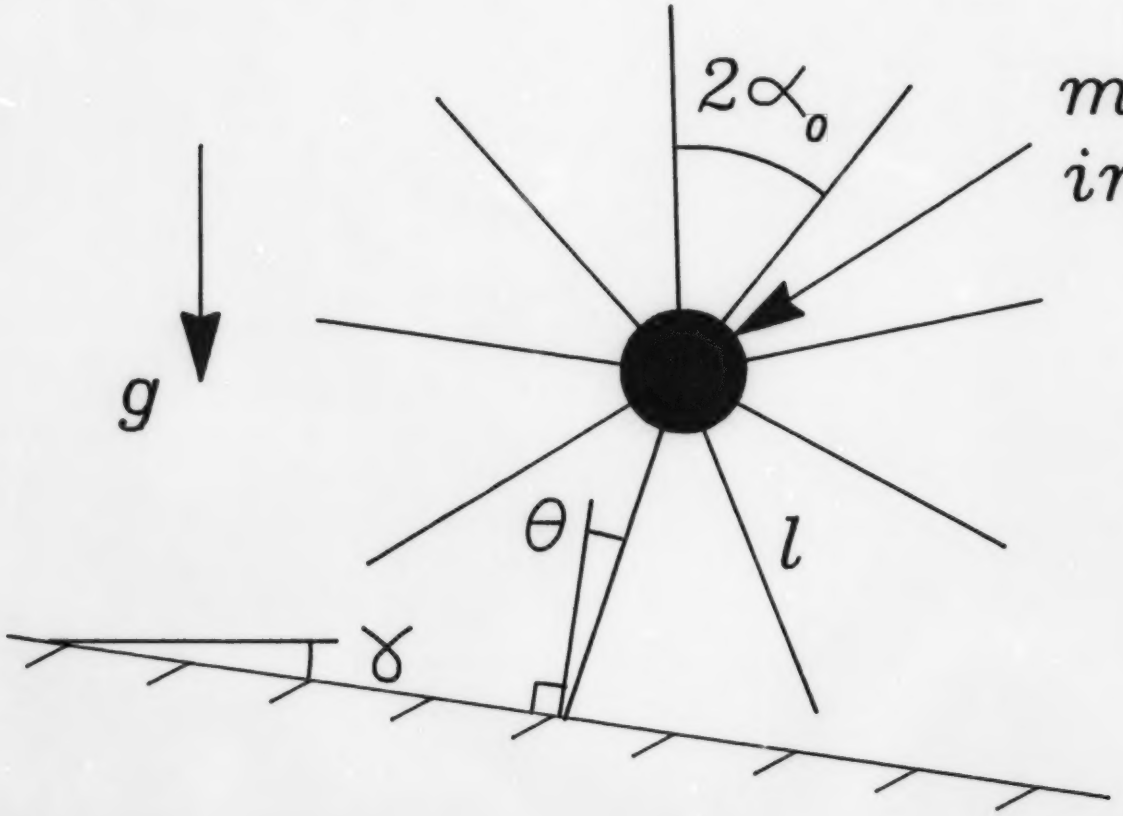

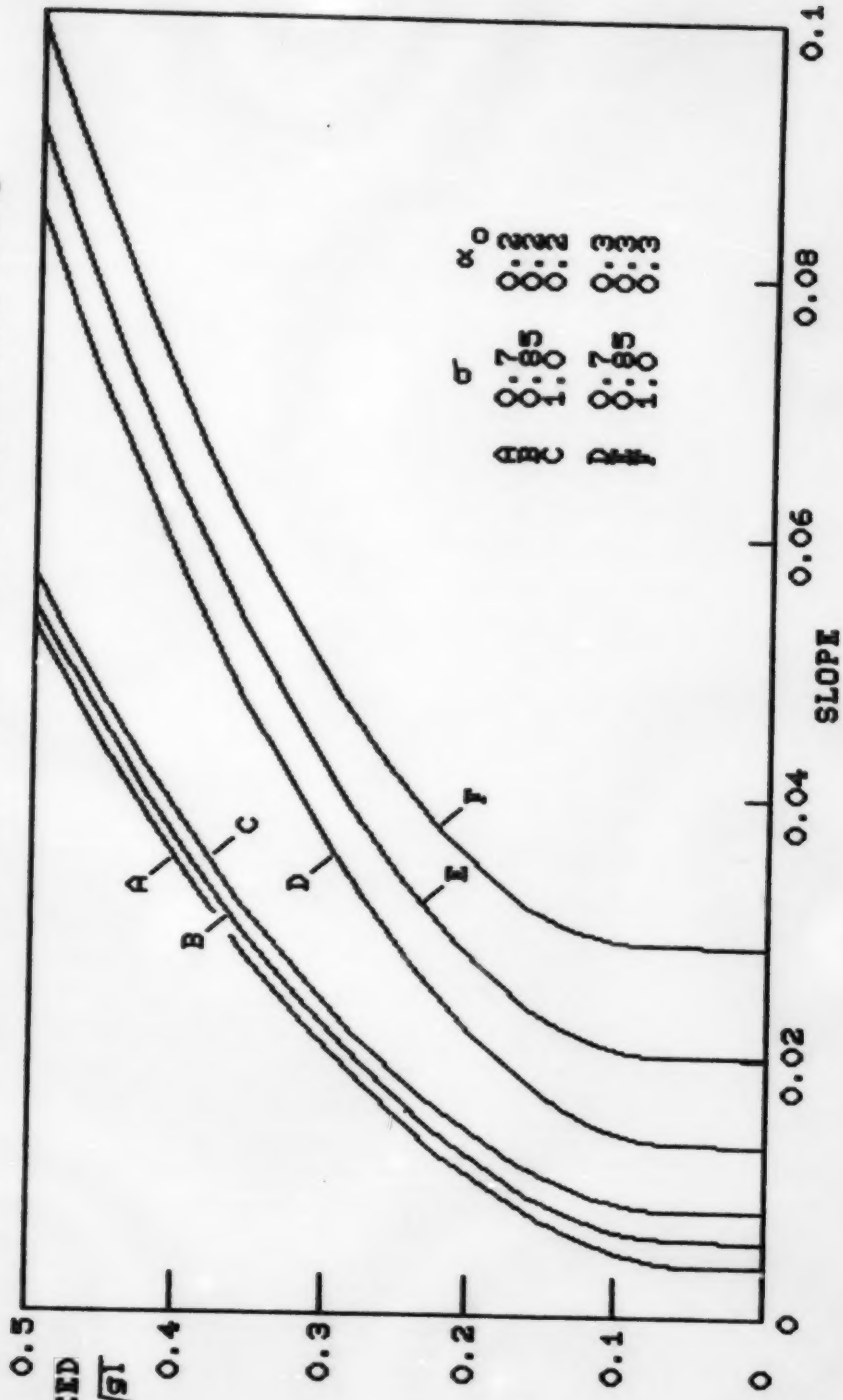

Figure 5. *Dimensionless forward speeds of various rimless wheels. As an example,* $\gamma = 0.02$, $\alpha_0 = 0.3$, $\sigma = 0.75$, $l = 0.5m$ *produces a forward speed of* $0.36m/s$ *in* $1g$.

Figure 6. *A "synthetic wheel." In its natural mode of motion it rolls just like an ordinary wheel. The free leg swings forward to synthesise a continuous rim.*

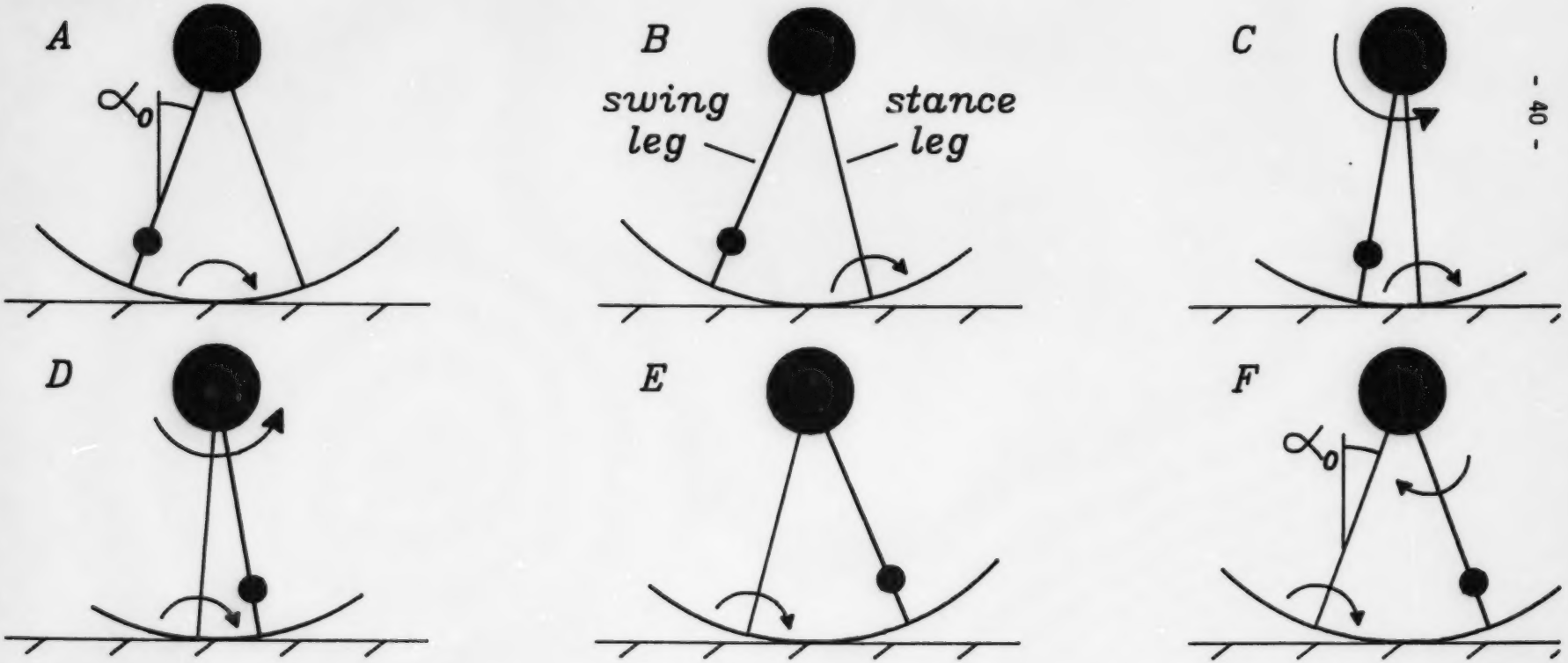

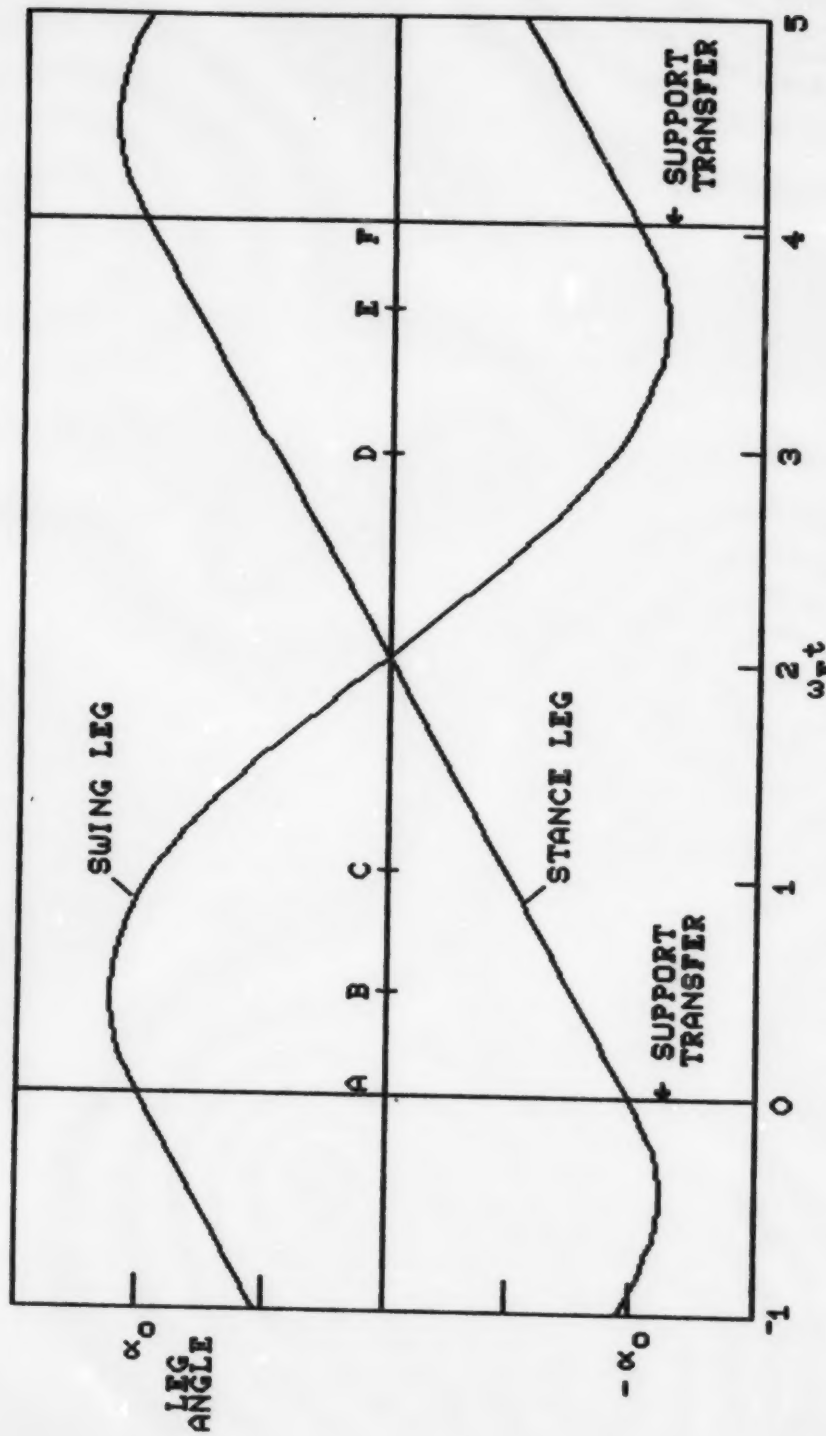

Figure 7. *One step of a synthetic wheel. Time is nondimensionalised by the pendulum frequency of the swing leg. Points corresponding to the frames in figure 6 are indicated by letter.*

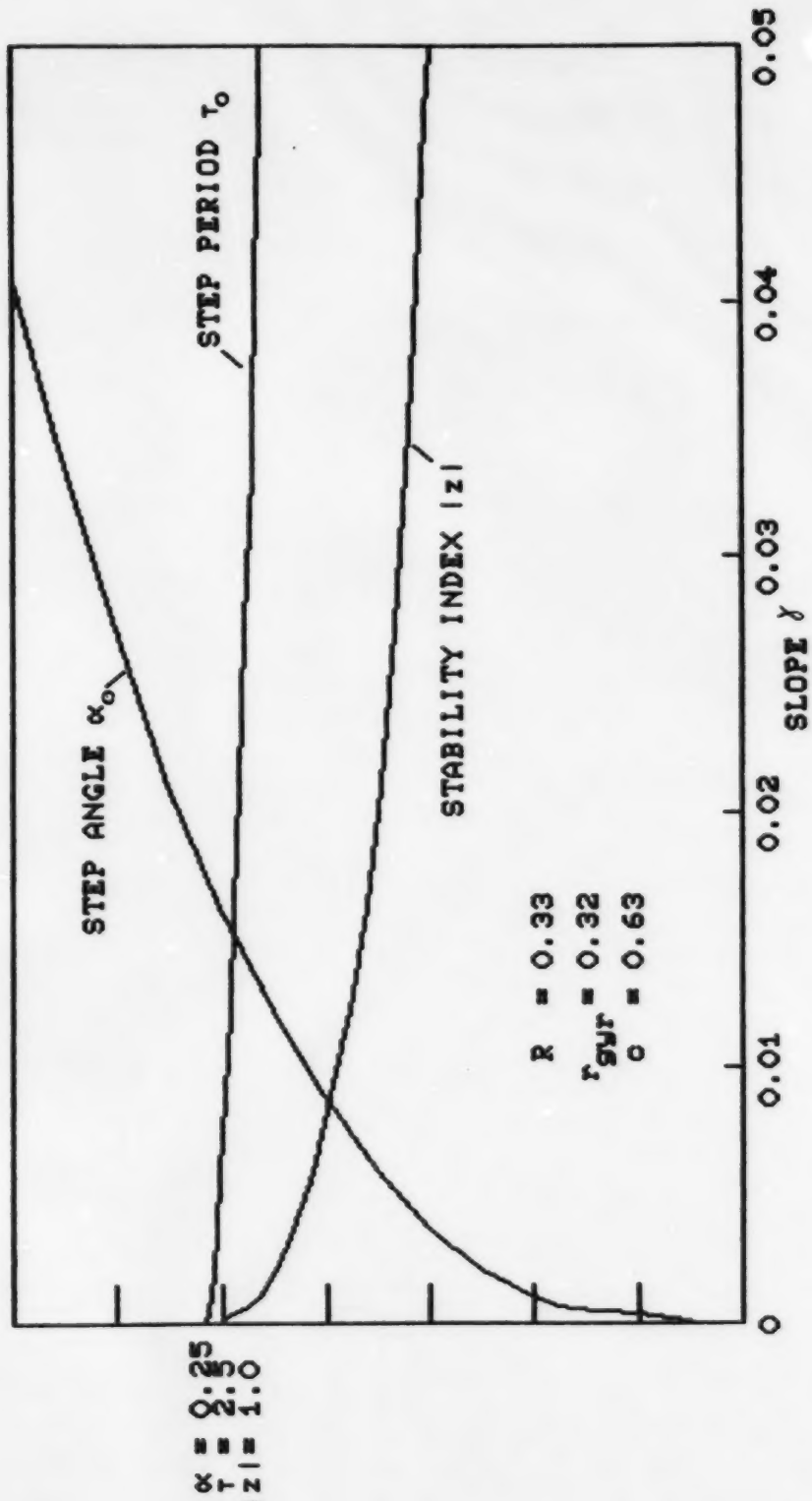

Figure 8. *Behaviour calculated for the test machine. Note that α_o is nearly proportional to speed, since the step period is nearly invariant with slope. The slope is equal to the weight-specific resistance.*

Figure 9. *Calculated effect of varying the foot radius of the test machine. Note that the resistance vanishes for R near unity, as for the synthetic wheel.*

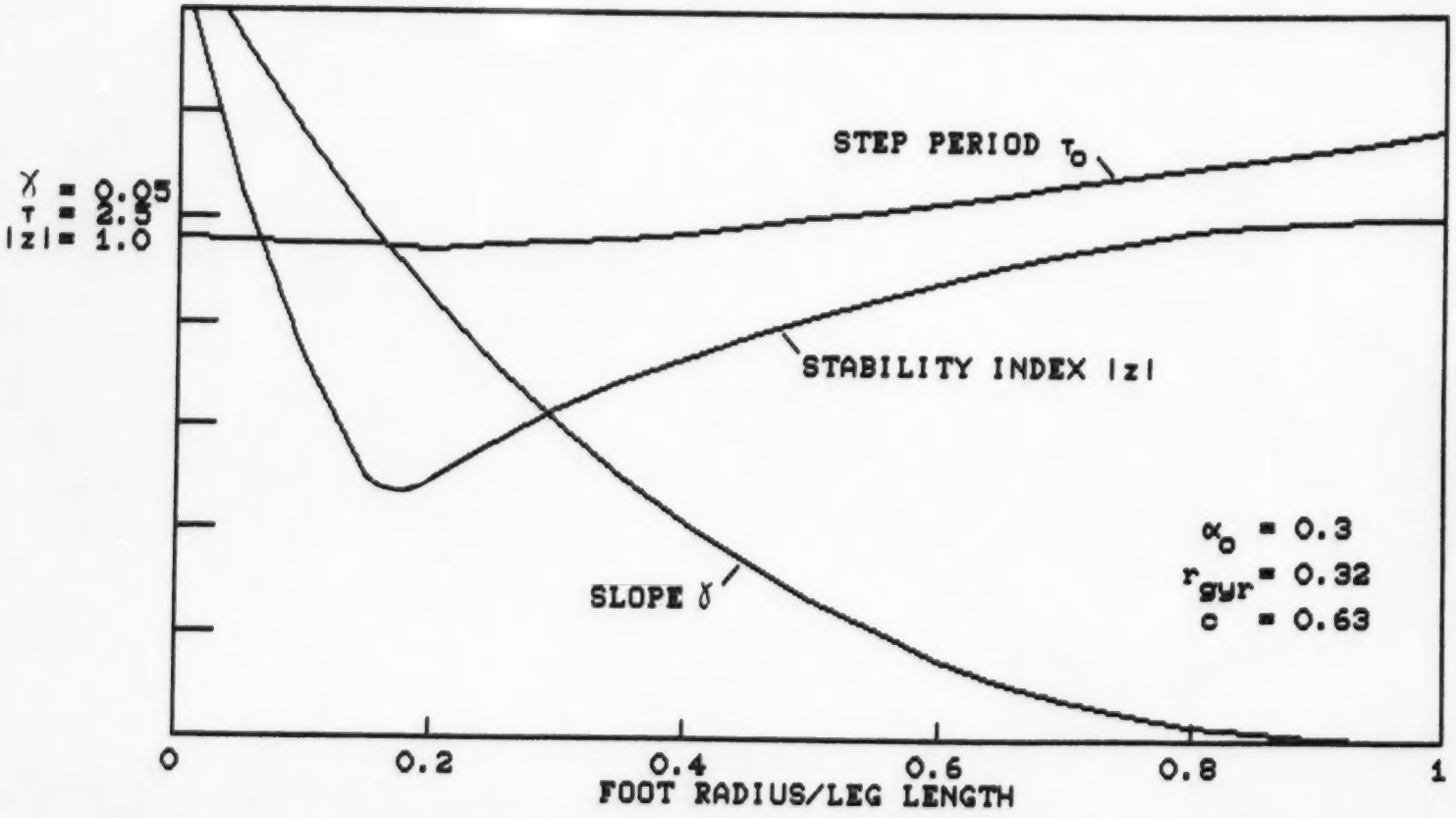

Figure 10. *Calculated effect of moving the mass centre along the leg. The range for stable walking can be extended to c = 0 by adding sufficient hip mass (which is zero in this example).*

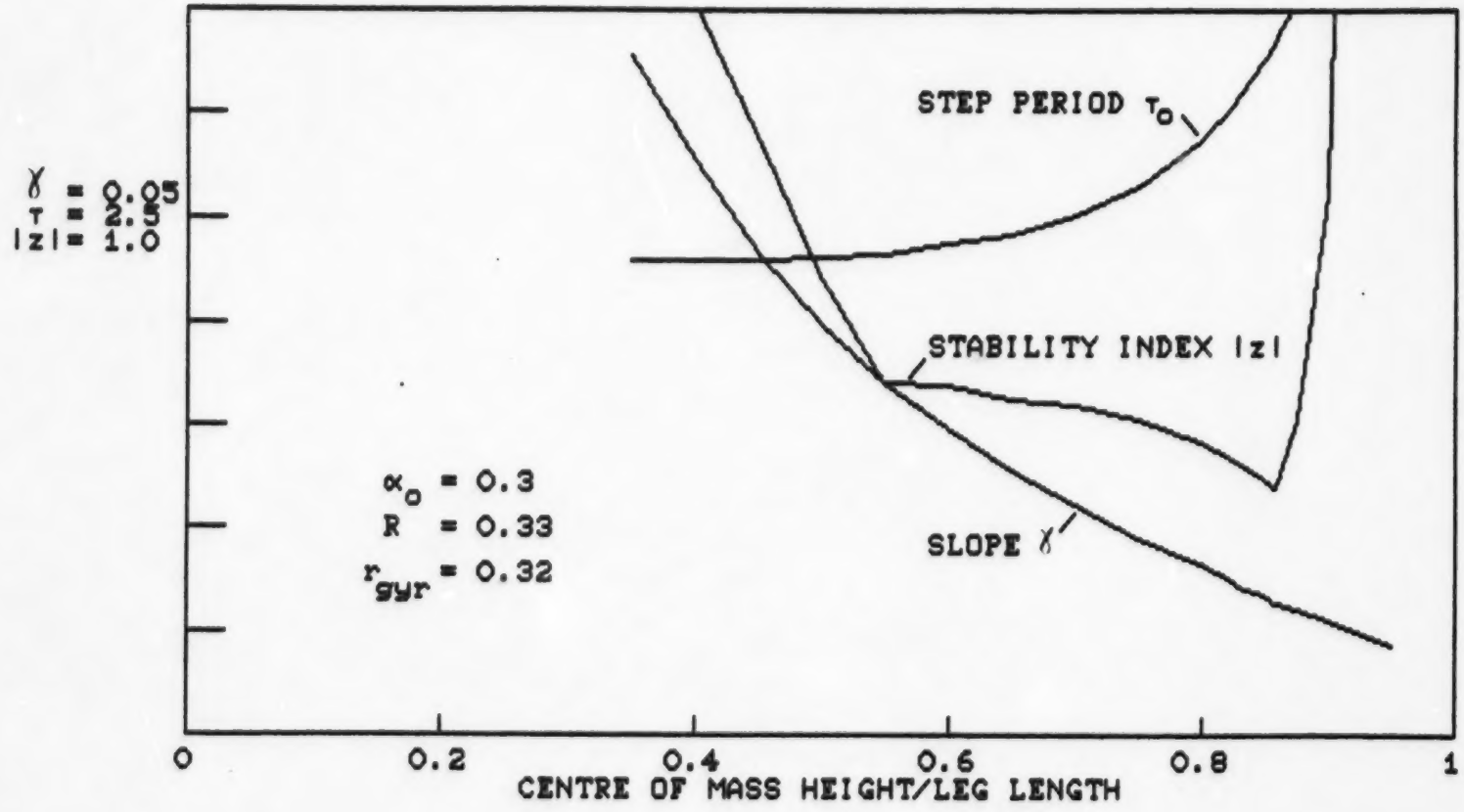

Figure 11. *Calculated effect of varying the leg's radius of gyration.*

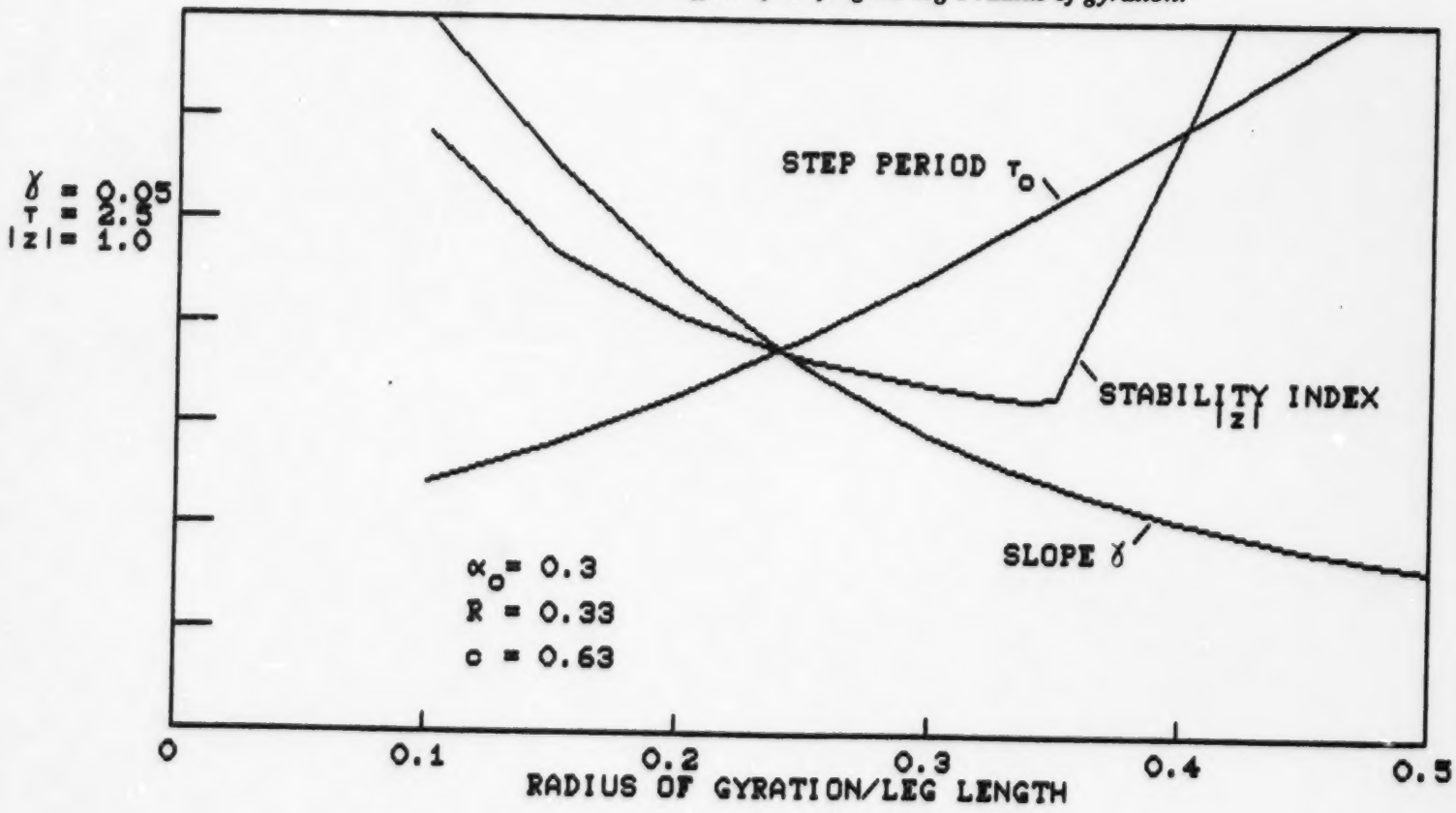

Figure 12. *Calculated effect of putting a body on the legs (which appears as a point hip mass in the equations of motion). In this example the walk is initially stable, and hardly changes despite addition of a large hip mass. With other parameter sets otherwise unsatisfactory dynamics can be improved by adding hip mass.*

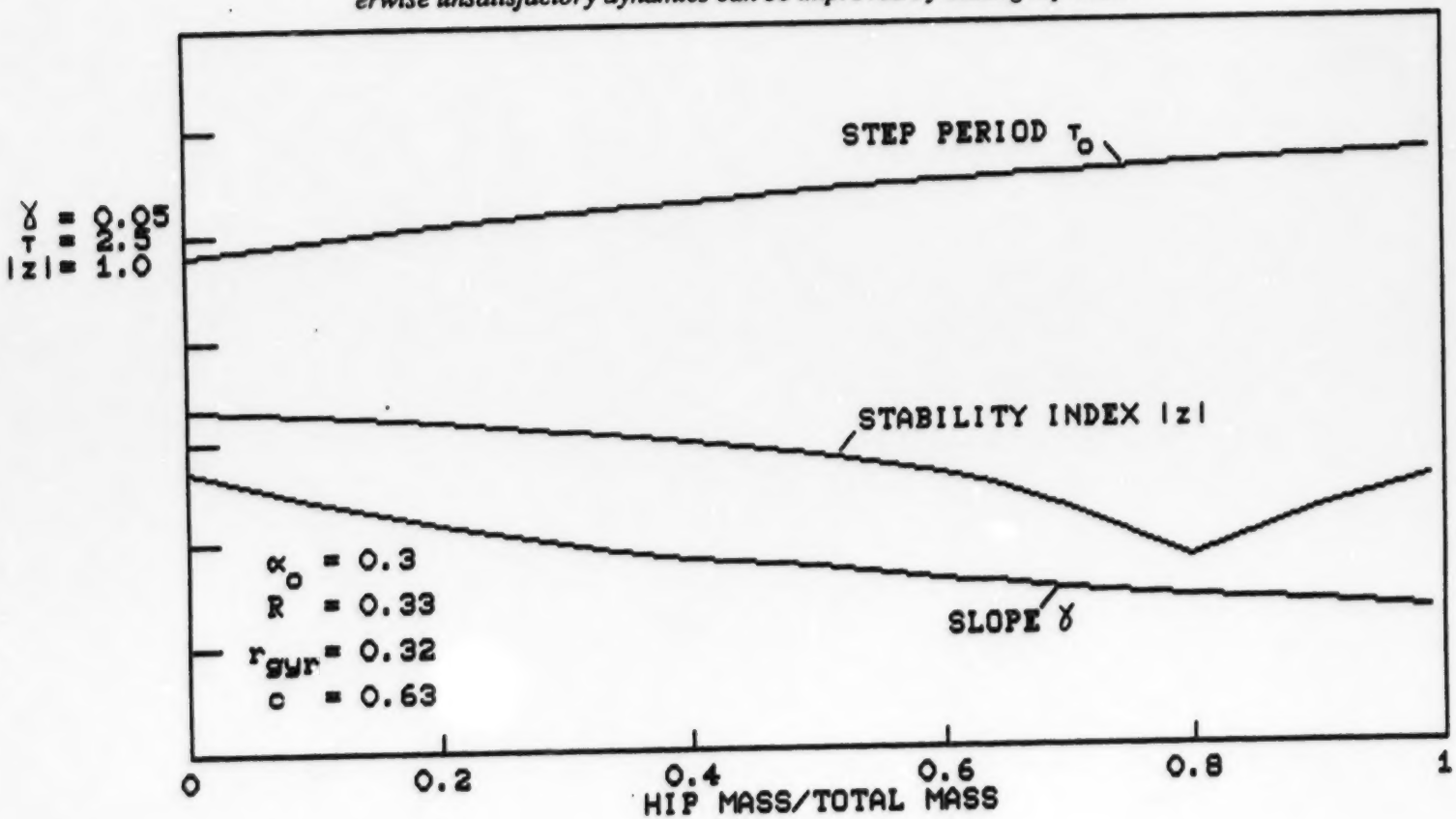

Figure 13. *A series of steps calculated for a machine with unmatched leg masses. The lighter leg takes the first step. The walk remains stable despite the mismatch, but the steady cycle is 4 steps long. With smaller mismatch the cycle repeats in only two steps.*

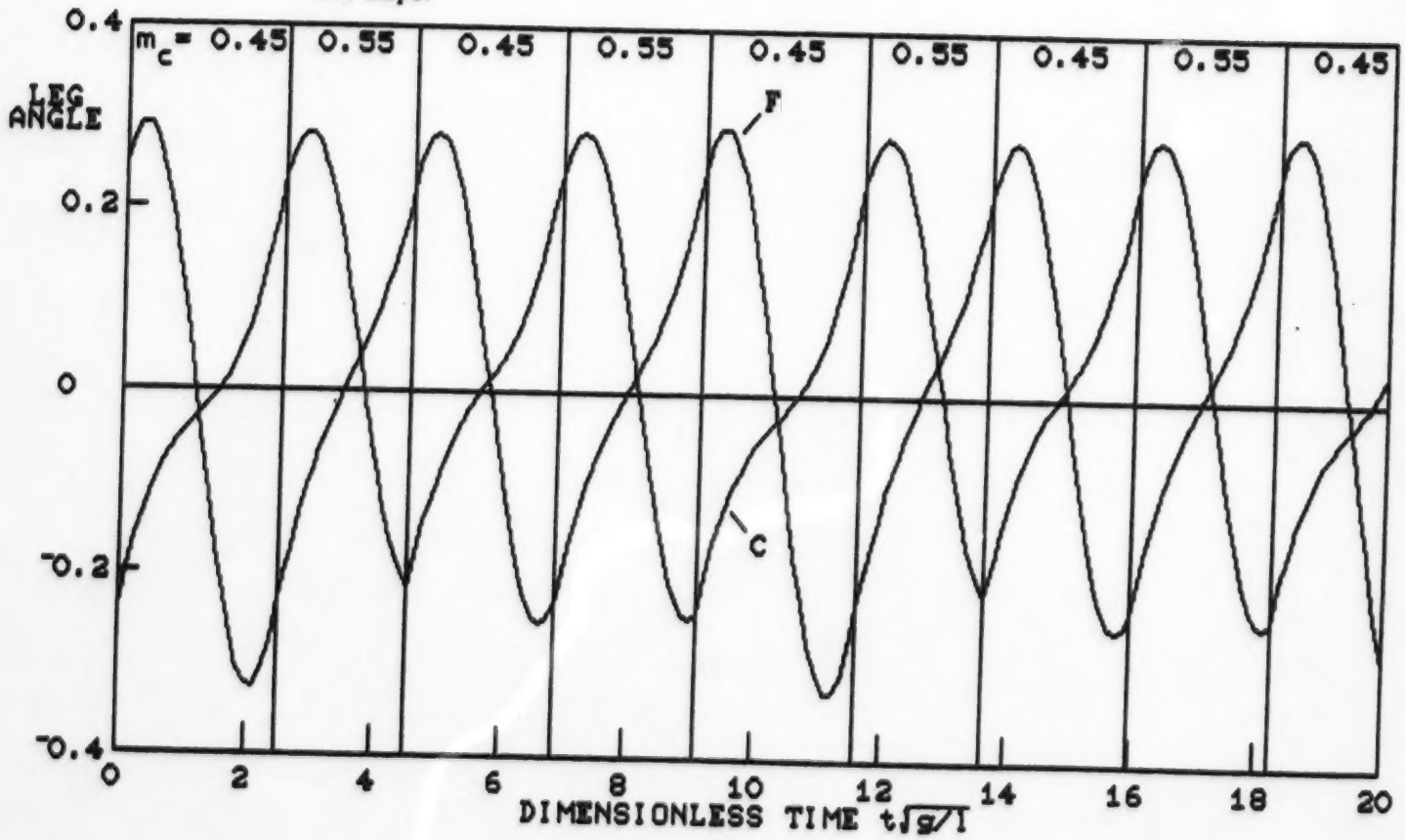

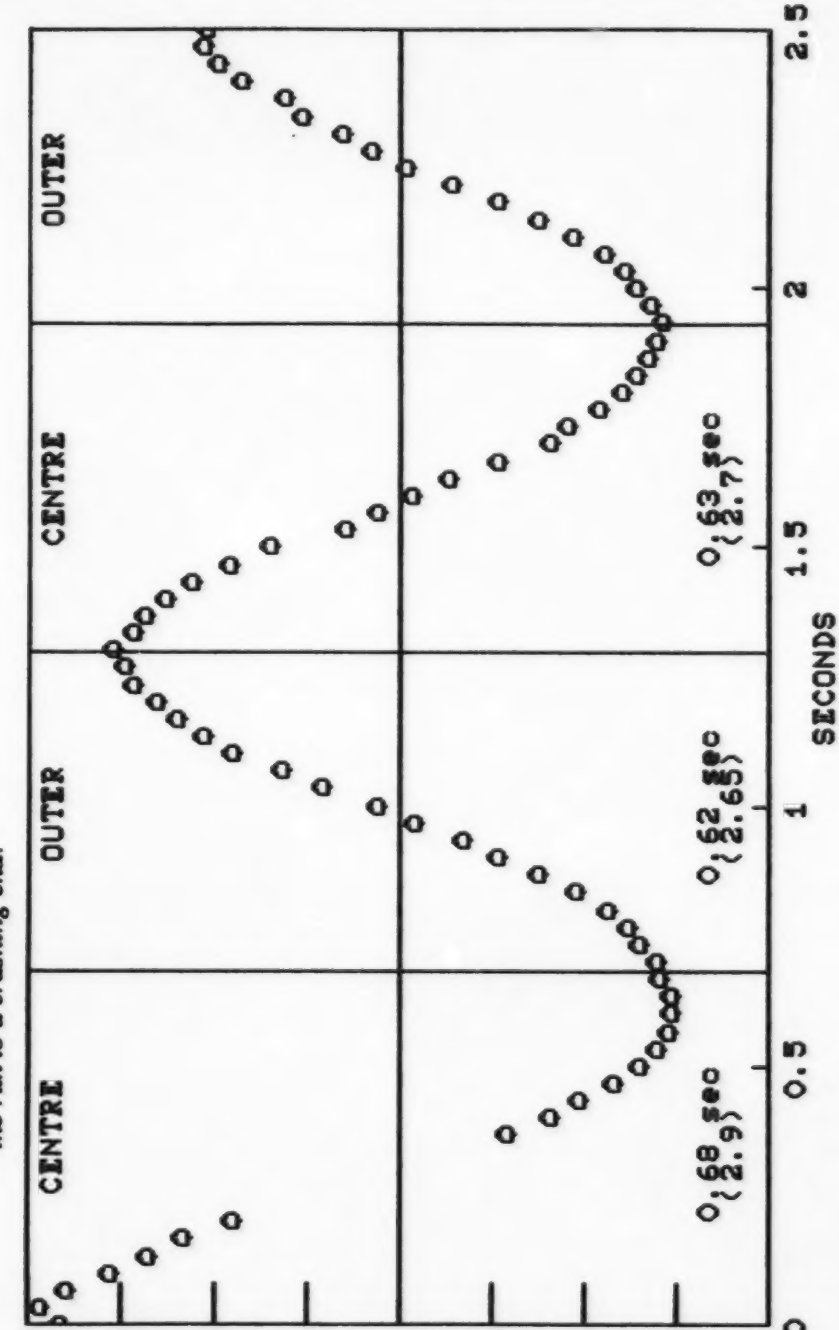

Figure 14. *A series of steps following manual starting of the test machine. The support leg for each step is noted at the top. The angle between the legs is defined as positive with the centre leg forward. Failure of the foot clearance mechanism brought the run to a crashing end.*

Figure 15. *A concept for fully passive walking in two dimensions. A knee joint is added to the original machine; it must be at or above the foot's centre of curvature so that flexure will clear the foot. The swing motion is ballistic after the spring provides a starting impulse. The foot is shortened on the heel side so that the support force will hold the stance knee against the stop.*

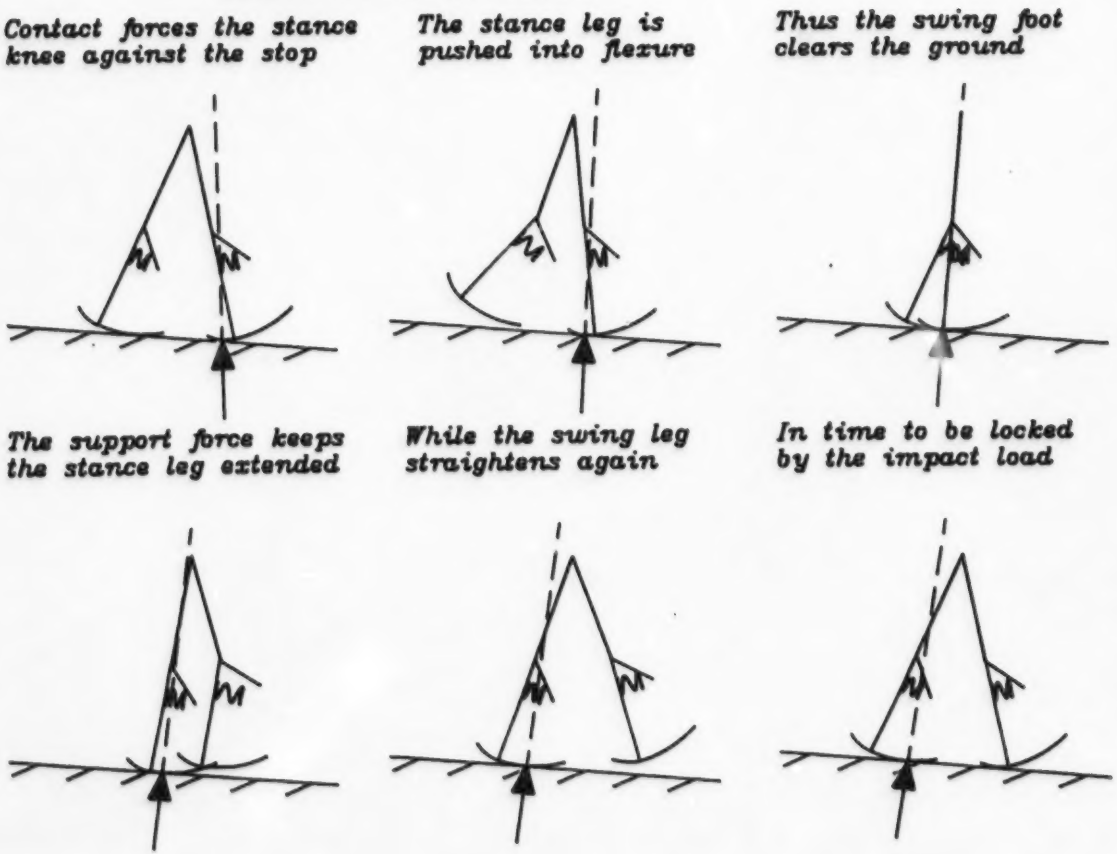
Contact forces the stance knee against the stop
The stance leg is pushed into flexure
Thus the swing foot clears the ground
The support force keeps the stance leg extended
While the swing leg straightens again
In time to be locked by the impact load

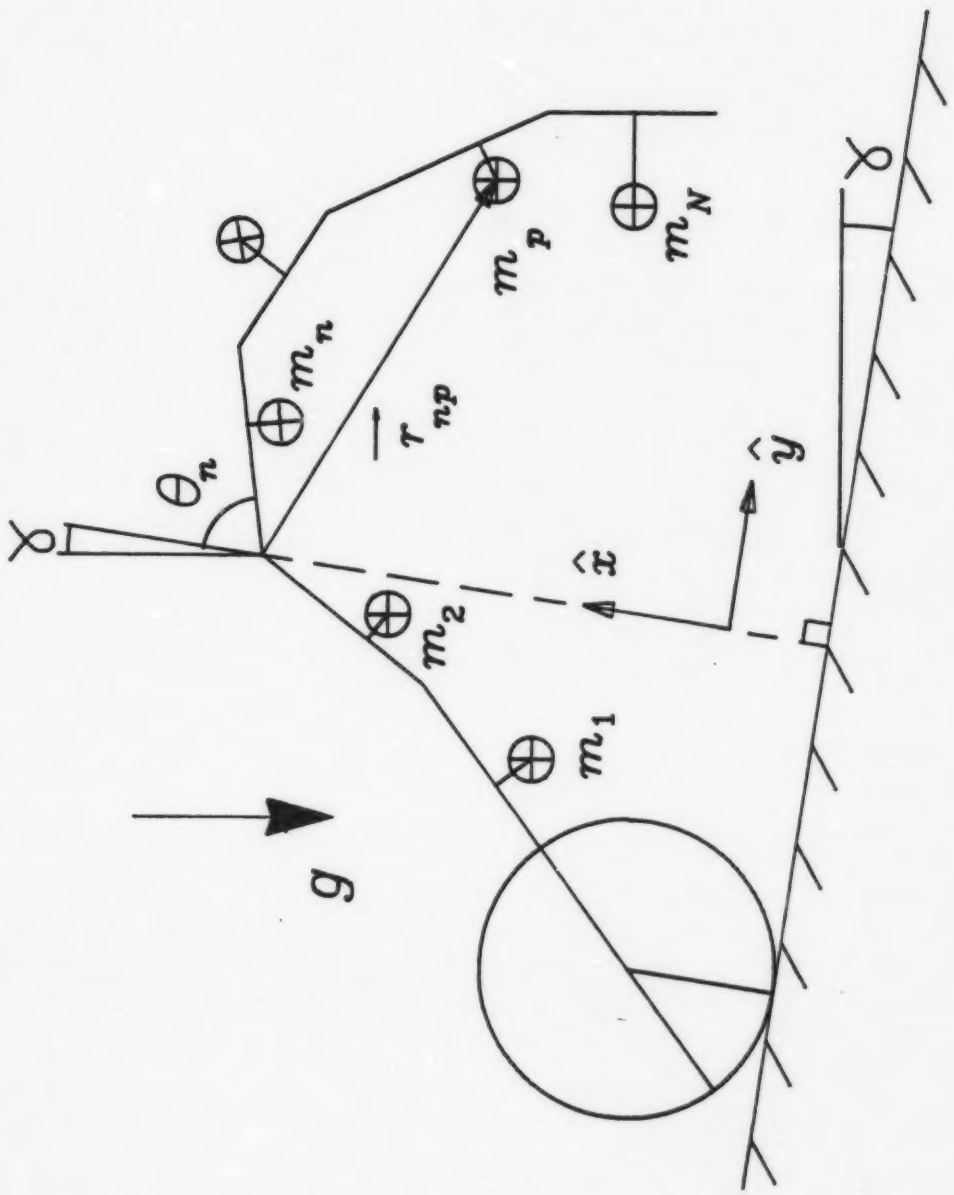

Figure 16. *Notation for an N-link, two-dimensional chain with rolling support.*

Figure 17. *Notation for individual links of the chain.*

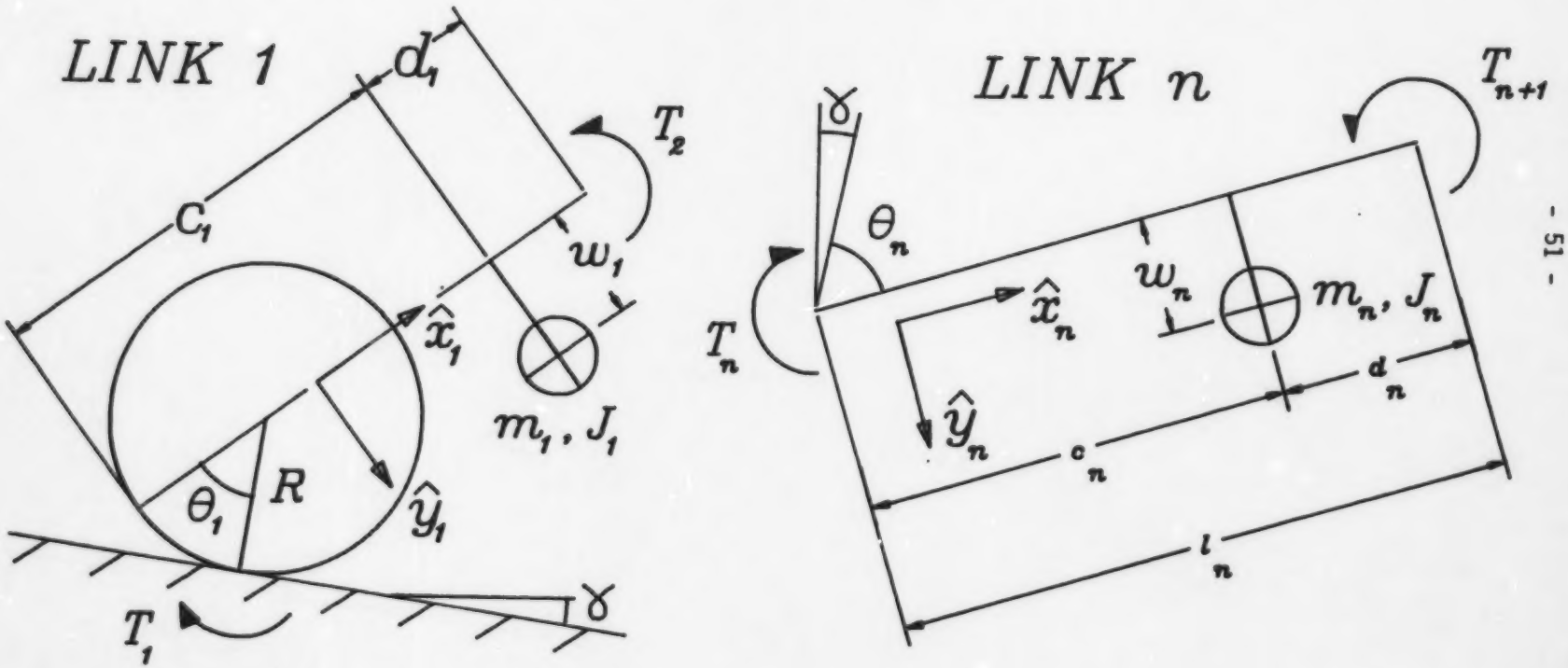

Centre for Systems Science

• Simon Fraser University established the **Centre for Systems Science** as a provincial centre for advanced study. The objective of CSS is twofold: coordinate and combine advanced systems research at SFU, and encourage application of research results within industry in order to further the technological development of British Columbia.

•CSS has assembled three research groups to streamline its efforts. The orientation of these groups is as follows: intelligent systems, microelectronics, and computer and communications systems. Because of shared research interests, this latter group merges with LCCR (**Laboratory for Computer and Communications Research**) for the publication of technical reports.

• CSS's three groups involve over 80 skilled faculty researchers principally from SFU's Schools of Engineering Science and Computing Science, but also draw substantially on Mathematics, Physics, Geography, Philosophy, Linguistics, Psychology, Communication, and Kinesiology.